INVESTIGATION OF 980-nm DIODE LASER PARAMETERS FOR SOFT TISSUE SURGERY

by

Yusuf Korkmaz

B.S., Electrical and Electronics Engineering, Boğaziçi University, 2003

Submitted to the Institute of Biomedical Engineering
in partial fulfillment of the requirements
for the degree of
Master of Science
in
Biomedical Engineering

Boğaziçi University
July 2006

ACKNOWLEDGMENTS

I would like to thank my supervisor Assist. Prof. Dr. Murat Gülsoy for his friendly guidance and contributions during the course of my thesis.

I would like to express my gratitude to Prof. Dr. İnci Çilesiz and Assoc. Prof. Dr. Hale Saybaşılı for their contributions to my thesis and for being a member of my thesis committee. I would like to thank Prof. Dr. İnci Çilesiz from Istanbul Technical University once more for lending the diode laser source used in experimentation.

I would like to thank Özgüncem Bozkulak and H. Özgür Tabakoğlu for their valuable suggestions and support through out my thesis.

This study was supported by TUBITAK Project 104M428.

I am also grateful to my mother, father, brother and lovely wife for their endless support and patience that made all of this work possible.

ABSTRACT

INVESTIGATION OF 980-nm DIODE LASER PARAMETERS FOR SOFT TISSUE SURGERY

Within 800 – 1064 nm spectrum 980 nm diode laser is very important because of the local absorption peak around 980 nm. This work was carried out to find the irradiation doses for maximum coagulation of soft tissue without carbonization. Lamb tissues (liver, heart and kidney) were irradiated with 980 nm diode laser. Coagulations were quantified in terms of diameter and depth measurements. Laser beam was applied in two different modes: Continuous wave and modulated in 250 ms on/off and 50 ms on/off cycles. Carbonization threshold for each mode (CW or modulated) were found. Maximum irradiances and maximum energy densities were recorded. For best proposed doses histological analyses performed and thermal alteration was observed. For modulated wave, the effect of the duration of the duty cycle was discussed. The comparison of tissue types was done and water content of each tissue was calculated by desiccation method. Maximum irradiances, maximum energy densities and water content were compared. The result of this research study is a step for understanding the characteristics of 980 nm diode laser for soft tissue surgery.

Keywords: 980-nm diode laser, lamb, soft tissue, surgery, parameter, dose, histology

ÖZET

YUMUŞAK DOKU CERRAHİ OPERASYONLARI İÇİN 980-nm DİYOT LAZER PARAMETRELERİNİN ARAŞTIRILMASI

Suyun 980 nm civarındaki yerel ışık soğurma tepesi nedeniyle diyot lazerin 800 – 1064 nm aralığında çok önemli bir yeri vardır. Bu çalışma, yumuşak dokuyu karbonize etmeden maksimum koagüle eden dozları bulmak için yapılmıştır. Koyun dokuları, karaciğer, kalp ve böbrek) 980 nm diyot lazere tabi tutulmuştur. Koagülasyon miktarları derinlik ve yüzeyin çapı olarak ölçülmüştür. Lazer ışını iki farklı şekilde verilmiştir: Sürekli lazer ışığı ve darbeli lazer ışığı. Darbeli lazer ışığı da iki farklı şekilde uygulanmıştır; 50 ms açık/kapalı ve 250 ms açık /kapalı. Her üç şekil için de karbonizasyon eşikleri saptanmış, maksimum güç yoğunluğu ve maksimum enerji yoğunluğu bulunmuştur. Önerilen en iyi dozlara tabi tutulan örneklerin histolojileri yapılmış ve termal bozulma gösterilmiştir. Darbeli lazer ışığı için açık/kapalı sürelerinin uzun ya da kısa olmaları tartışılmıştır. Her üç doku için de *in vitro* olarak içerdikleri su miktarları hesaplanmış ve bu bilgiler ışığında deney sonuçları karşılaştırılmıştır. Bu çalışma 980 nm diyot lazerin yumuşak doku cerrahi operasyonlarında gösterdiği özellikleri anlamak ve belirlemek açısından bir adımdır.

Anahtar Sözcükler: 980-nm diyot lazer, koyun, yumuşak doku, parametre, doz, histoloji

TABLE OF CONTENTS

LIST OF FIGURES

LIST OF TABLES

LIST OF SYMBOLS

μ_a	Light absorption coefficient
λ	Wavelength
g	Anisotropic scattering coefficient
W	Watt
J	Joule
mm	millimeter
ms	millisecond
gr	gram

LIST OF ABBREVIATIONS

HpD	Hematoporphyrin Derivative
PDT	Photodynamic Therapy
LLLT	Low Level Laser Therapy
Nd:YAG	Neodymium Yttrium Aluminium Garnate
CW	Continuous Wave
H&E	Hematoxylin and Eosin
PFA	Paraformaldehyde
PBS	Phosphate Buffered Saline

1. INTRODUCTION

Laser technologies have a rapidly increasing importance in biotechnology. Since the usage of sunlight in ophthalmology to burn retina, many other applications of lasers are developed. Today laser is not only a medical equipment for ophthalmology but is very useful and effective in other medical areas. For example “green light” is the easiest and the fastest way to solve prostate problems. Another example is the skin resurfacing by laser application. These examples may continue.

Laser tissue interaction is a very wide subject since the wavelength, application parameters (power, mode of operation, exposure time…) and optical properties (absorption, scattering, transmission) of tissue differs so much. Therefore research on different tissues with different type of lasers and dosimetry parameters continues.

Bozkulak and Tabakoğlu (2004) [1] studied on the effects of 980-nm diode laser for brain surgery. This work was carried out to examine the extent of thermal changes and the recovery process of laser induced brain lesions. As a result, the 980-nm diode laser system has a remarkable ablating ability with minimal thermal damage the nearby tissue.

Ware and Boor (1999) [2] studied slow intramural heating with diffused laser light (805-nm) to show that catheter ablation of postinfarction ventricular tachycardia may be limited by insufficient myocardial coagulation or excessive endocardial or epicardial damage. The research showed that slow, volumetric and direct intramyocardial heating induces large, deep lesions without hazardous tissue damage which might be a safer cure than the present techniques.

Germer and Albrecht (1999) [3] studied diffusing fiber tip for the minimally invasive treatment of liver tumours by interstitial Nd:YAG laser (1064-nm) coagulation.

The results showed that tissue can be interstitially coagulated with special laser applicators in a single laser session under *in vitro* conditions.

White and Chaundhry (1998) [10] studied Nd:YAG and CO_2 laser therapy of oral mucosal lesions. The results showed that laser excision was well tolerated by patients with no intraoperative or postoperative adverse effects. All patients healed with no loss of function postsurgically. CO_2 and Nd:YAG lasers are successful surgical options when performing excision of benign intraoral lesions.

These studies show that there are many laser types used in surgery. Within these types diode lasers are compact, portable and also are cheaper than the other ones. The 980-nm diode laser has another advantage that water has an absorption peak around 980-nm. Therefore 980-nm diode laser may be a good alternative to Nd:YAG for surgical use.

1.1 Aim of Study

This project's objective is to experiment lamb liver, heart and kidney at 980-nm with a diode laser to find appropriate parameters (continuous or modulated, power, exposure time…) to coagulate the target with minimum damage of nearby tissue. Moreover the modulation types will be compared under same conditions.

The aim of this project is to determine the optimum parameters for coagulating the desired tissue volume for each tissue type without damaging the surrounding tissue.

2. BACKGROUND

2.1 Laser-Tissue Interaction

Laser tissue interaction mechanisms are a function of wavelength, power, and pulse duration. The penetration depth of the laser light depends on the optical properties of the tissue at the selected wavelength. There are currently five interaction mechanisms associated with laser treatment of patients.

2.1.1 Photothermal Effect

Photothermal mechanisms are based on the volumetric rate of heat production (W/cm^3) that occurs when laser light is absorbed by water and tissue chromophores like hemoglobin and melanin. Depending on the duration and peak value of the tissue temperatue achieved, different effects like coagulation, vaporization, carbonization and melting may be distinguished [4].

2.1.2 Photochemical Effect

Laser irradiation can react with photosensitizing chemicals that are injected intravenously into human body. Such a photochemical reaction can lead to an irreversible damage of tissues. Photosensitizers, such as hematoporphyrin derivative (HpD), which accumulate in tumors, are being used for treatment of cancer with a technique called photodynamic therapy (PDT). Photochemical interactions take place at very low power densities and long exposure times [4].

2.1.3 Photoablation

The material is decomposed when exposed to high intense laser irradiation. Typical power parameters are 10^7-10^8W/cm^2 and typical exposure time is in the nanosecond range. The ablation depth is determined by the energy given but there is a saturation point. Main clinical advantages of this interaction type are, precision of the etching process, predictability and lack of thermal damage to adjacent tissue[5].

2.1.4 Plasma-Induced Ablation

By plasma- induced ablation, very clean removal of tissue can be achieved without any thermal or mechanical damage. When power densities exceed 10^{11}W/cm^2 in solids and fluids optical breakdown occurs. It makes energy deposition possible not only in pigmented tissue but also in nominally weakly absorbing media because of the increased absorption coefficient of the induced plasma [5].

2.1.5 Photodisruption

If breakdown occurs inside soft tissues or fluids, cavitation and jet formation may additionally take place. At higher pulse energies shock waves and other mechanical side effects become more significant and might even determine the global effect upon the tissue. Cavitation is an effect that occurs when focusing the laser beam not on the surface of a tissue but into the tissue[5].

2.2 Photothermal Interaction

One of the most important laser tissue interaction type is the photothermal interaction which has a a wide clinical usage. Due to the exposure time, power and modulation type (CW or modulated) different effects such as coagulation, vaporization, carbonization and melting may be achieved as graphed in Figure 2.1.

2.2.1 Hyperthermia

The first mechanism by which tissue is thermally affected can be attributed to conformational changes of molecules. Bond destruction and membrane alterations are observed. Hyperthermia ranges approximately between 42-50^{o}C.

2.2.1 Coagulation

In a histologic section, the coagulated area can be easily detected by staining the tissue with hematoxylin and eosin. Coagulated tissue appears significantly darker than other tissue. During this irreversible process, temperature reach at least 60^{o}C, and coagulated tissue becomes necrotic. In the following figures the examples for coagulated tissue and the histological appearance of coagulated tissue for each tissue type are illustrated

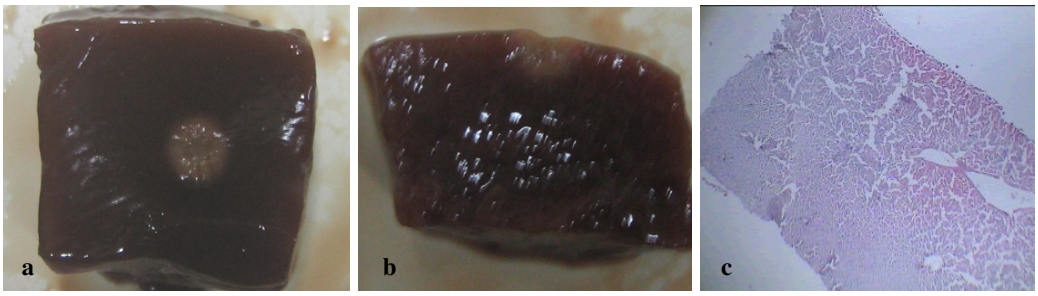

Figure 2.1 **Coagulated tissue samples for liver** a. **Surface.** b. **Inside.** c. **Histological appearance.**

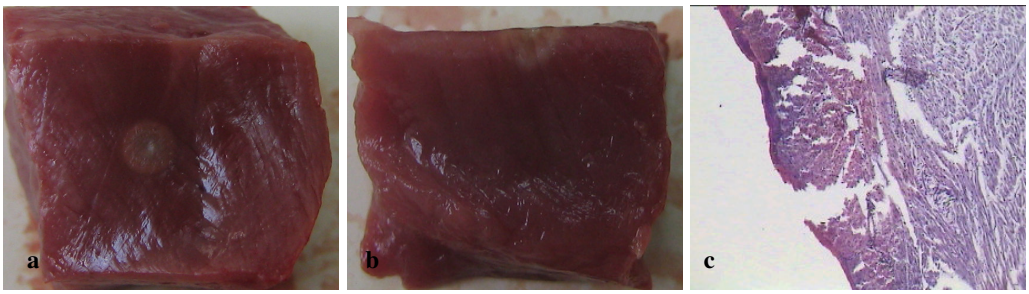

Figure 2.2 Coagulated tissue samples for heart **a.** Surface. **b.** Inside. **c.** Histological appearance.

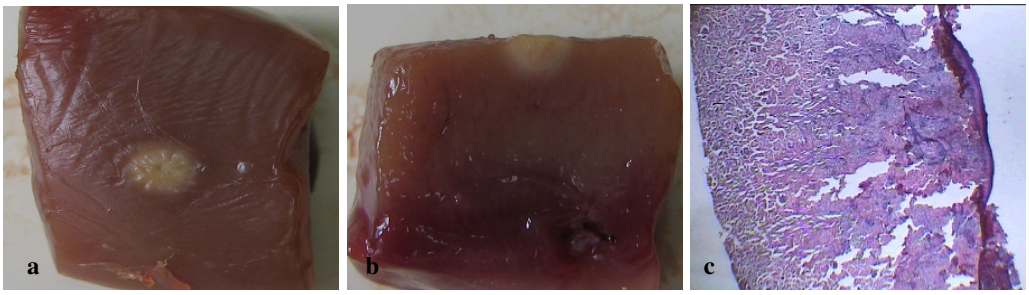

Figure 2.3 Coagulated tissue samples for kidney **a.** Surface. **b.** Inside. **c.** Histological appearance.

2.2.3 Vaporization

Water absorbs the laser wave which leads to vaporization. During vaporization it tries to expand in volume, the pressure increases and finally localized microexplosions occur. Vaporization is sometimes referred as a thermomechanical effect due to the pressure build-up involved. The resulting ablation is called thermal decomposition.

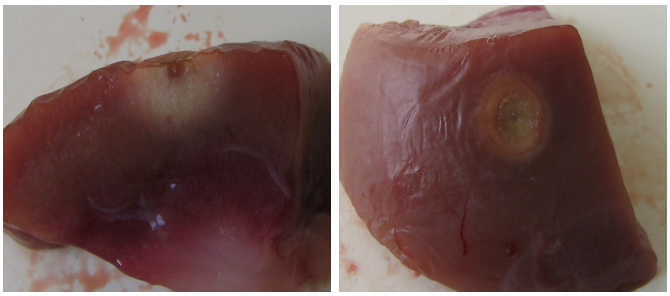

Figure 2.4 Vaporization examples for kidney samples.

2.2.4 Carbonization

When too much energy is applied to the tissue, the local temperature of the exposed tissue drastically increases and carbonization occurs. At temperatures above approximately 100^{o}C, the tissue starts to carbonize, carbon is released, leading to a blackening colour. For medical laser applications, carbonization should be avoided in any case, since tissue already becomes necrotic at lower temperatures. Thus, carbonization only reduces visibility during surgery. In the following figures carbonized tissue examples are shown.

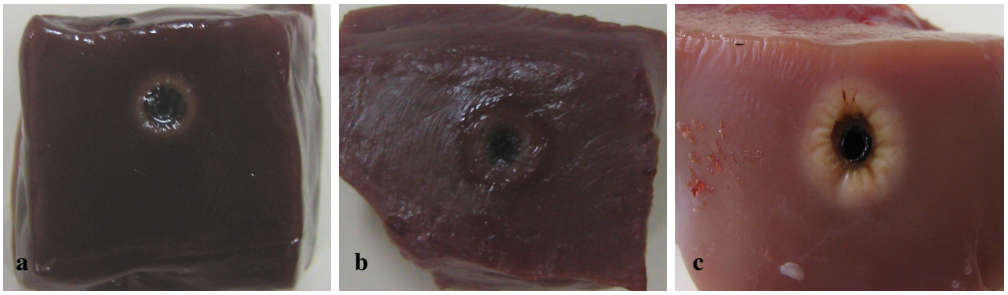

Figure 2.5 Carbonized samples. **a.** Liver. **b.** Heart. **c.** Kidney.

2.2.5 Melting

The temperature must have reach a few hundred ^{o}C to melt the tissue. Cracks may be seen (especially on tooth surface) originated from thermal stress induced by a local temperature gradient across the surface. Obviously, the pulse duration of a few microseconds may be enough to enable a sufficient increase in temperature[5].

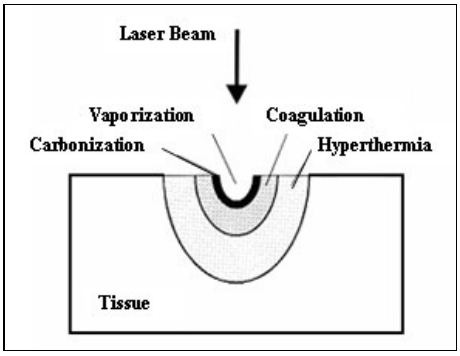

Figure 2.6 Order of the photothermal effects of a laser on a tissue [5].

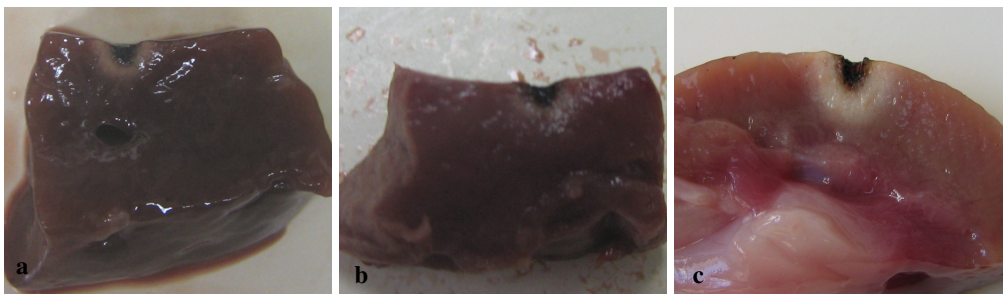

Figure 2.7 Examples for the photothermal effects of laser. **a.** Liver. **b.** Heart. **c.** Kidney.

2.3 Heat and Heat Transfer

Whether created by electrosurgical electrodes or laser devices, cutting, ablation and photocoagulation are caused by heat. The advantages of these high energy modalities lie in their ability to effectively create and localize this heat enough to produce desired surgical effects with associated hemostasis. Laser effects may be more highly localized than can electrosurgery.

The transfer of heat from one object to another occurs through one or more of three basic mechanisms: conduction, convection and radiation. Lasers are used in one of two ways to generate heat – either “non-contact” methods which rely on radiation transfer, or contact methods which rely on conduction of heat.

Conductive heat transfer is the flow of heat energy in matter as a result of molecular collisions. In other words, if you touch a hot object to tissue it can burn it through direct conduction of heat.

Convection is the second method of heat transfer and involves larger scales quantities of matter than conduction, such as seen in heating of gases and liquids in boiling a pan of water. Convection is what carried away the excess heat from the incision site through generation of steam. If the laser is used to dissect in a manner which is too slow to allow any generation of steam, then heat will build up in the tissue and conduct into lateral tissues. This usuallly occurs when the laser is used at such painfully low powers that vaporization cannot immediately proceed, and the device just wallows and burns in tissue. Adequate power levels for clean vaporization will generate the required steam envelope around the device and carry away excess heat.

Radiation heat transfer is the primary mechanism of non-conduct laser modalities. This involves the transfer of thermal energy by electromagnetic waves. Materials do not have to touch to transfer heat this way. Heat may even be transmitted across a vacuum by radiation since it does not depend on the presence of matter [6].

2.3.1 Heat Effects

There is no measurable effects of heat for the next 5^{o}C above the body temperature. As the temperature increases hyperthermia is seen. If this condition lasts for several minutes it may turn to an irreversible process and the cell undergo necrosis. Beyond 50^{o}C enzyme activity reduces which causes a decrease in energy transfer within the cell. At 60^{o}C, denaturation of proteins leads to necrosis of cells and coagulation of tissue. At 100^{o}C water molecules start to vaporize which is advantageous, since water carries away the excess heat preventing increase in the temperature of adjacent tissue. Carbonization takes place at temperatures exceeding 100^{o}C , blackening of adjacent tissue and smoke visualized. Beyond 300^{o}C depending on the tissue melting can occur [5].

2.4 Diode Lasers

Developed in 1972, semiconductor diode lasers have progressed tremendously. Engineering and commercial specifications have allowed advancement of devices with wavelengths varying from approximately 635 to 980 nm. In the 1990s, diode lasers radiating in the near IR region (800-980nm) became commercially available. Their light weight, portable sizes, lower cost, longer operating life and better operating conditions make them attractive for medical applications. Diode lasers are semiconductor electronic devices, somewhat like a transistor. Laser light output is generated when electric current is passed through the diode. Individual diodes emit light from the edge of a wafer or from their surface. Standard single-emitter diodes can be combined on the same semiconductor chip to achieve very high output power from a device that is still very small. High-power diode lasers generate laser emission with an electrical-to-optical conversion efficiency of 30% to 50%, making them the most efficient lasers available. These direct diode laser systems collect diode emission and channel it onto tissue using an appropriate delivery system [6]. Coupling diode laser energy directly to fiberoptic delivery devices is a tremendous advantage when considering endoscopic application and minimally invasive surgical techniques.

These type of lasers produce laser light intrinsically and do not require the internal systems of gas or crystal types of lasers. Diode lasers may produce lights of various colours, depending on the particular diode, but most produce infrared light of very low power. The development that is occuring is in the expansion of wavelengths to the visible light spectrum and power increase up to several watts. Already arrays of diodes have been joined together to produce infrared surgical units of up to 100 watts in power. These are used in conjunction with contact types of fibers for hemostatic dissections or urologic procedures [7]. Other low powered units are used as ophthalmic photocoagulators, or for Low Level Laser Theraphy (LLLT), and in hair removal procedures.

The wavelengths of the diode and Nd:YAG lasers penetrate comparative depths into tissue because they are most absorbed by melanin, hemoglobin, and darker pigments that do not usually occur on the surface. The concentration of these or other darker pigments determines the penetration at a given energy level. Nonpigmented tissue, such as cornea, absorbs none of the energy, whereas a pigmented melanoma absorbs a great deal of the energy. A caveat to this comes with the 980-nm diode laser, which has increased water absorption compared with the 810-nm diode and the 1064-nm Nd:YAG laser ($\mu_a(H_2O, 980\text{-nm})=0.430cm^{-1}$, $\mu_a(H_2O, 810\text{-nm})=0.023cm^{-1}$, $\mu_a(H_2O, 830\text{-nm})=0.029cm^{-1}$, $\mu_a(H_2O, 910\text{-nm})=0.073cm^{-1}$) and produces an efficient surface effect [8]. Subsurface, nonpigmented tissue, such as myelin, which may ordinarily have been minimally affected by these wavelengths, could be at higher risk with the 980-nm diode laser.

The low power diodes are sufficient for ophthalmic use. The trend will be to replace the complicated and expensive ophthalmic laser systems with these portable lasers. Until a full range of colours are available however, they will not totally replace ion lasers for ophthalmology. They will also see use in photodynamic therapy as a light source to activate photosensitizing drugs. Furthermore there are researches on tissue welding by 980 nm diode laser.

Table 2.1

The absorption coefficients (μ_a , cm^{-1}) for water, hemoglobin and melanin are given for wavelengths (λ) in the visible to infrared region. The larger the coefficient value, the better the wavelength is absorbed by the substance [6].

Laser	λ (nm)	Water μ_a	Hemoglobin μ_a	Melanin μ_a
KrF	248	0.0168	586	8600
XeCl	308	0.005	307	4800
XeF	351	0.002	635	2677
Argon	514	0.003	156	780
KTP	532	0.004	203	630
HeNe	633	0.003	27	345
Diode	640	0.003	23	332
	680	0.004	12	269
	720	0.016	7	221
	760	0.026	7	183
	780	0.023	6	167
	810	0.023	4	147
	830	0.029	4	135
	910	0.073	4	98
	980	0.430	2	76
Nd:YAG	1064	0.120		57
Ho:YAG	2120	27		
Er:YAG	2940	12,000		
CO_2	10,600	800		

3. METHODOLOGY

3.1 Experimental Setup

System consists of a microcontroller unit, high power 980-nm diode laser (Opto Power OPC-D010-980-FCPS), SMA connector (Opto Power OPC-OC01S/N:648-437) and PC based user interface program as seen in Figure 3.1. In figure there is also the SMA Connector for the connection between the laser and the fiber cable. A 400-µm silica coated optical fiber (Spindler–Hoyer, Göttingen, Germany) was used.

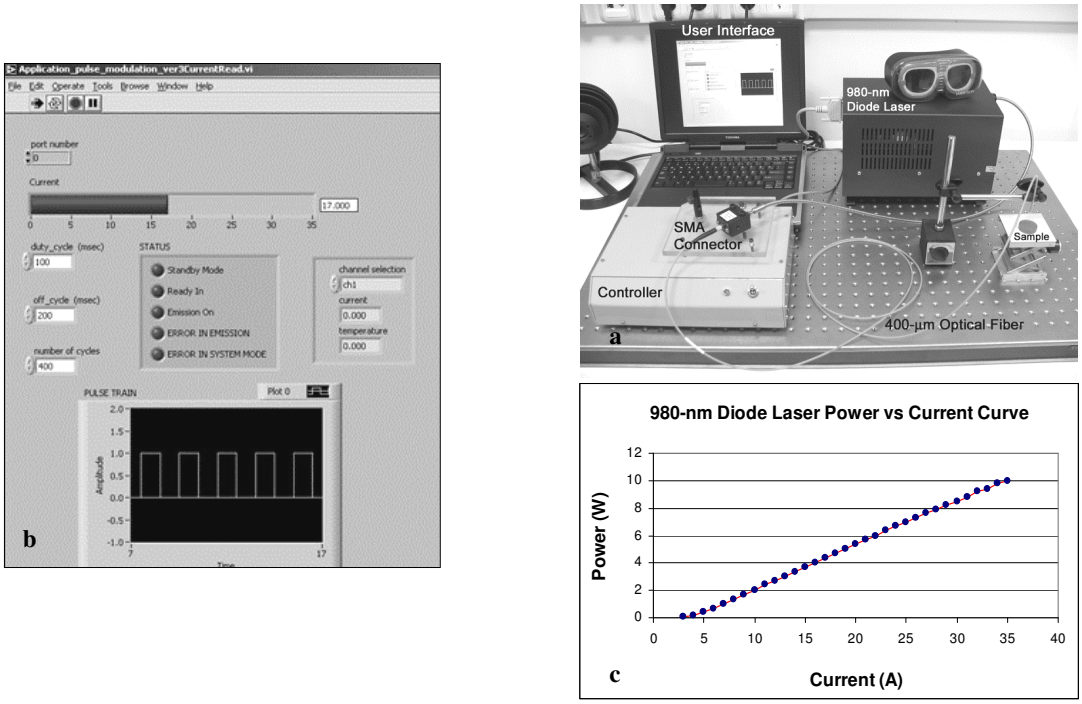

Figure 3.1 **a.** Experimental setup, diode laser, microcontroller, user interface, SMA connector and fiber optic cable. **b.** User interface. **c.** 980nm Diode Laser Power vs Current Curve graph.

980-nm diode laser (Class IV) gives maximum output power of 10W and this power is obtained by changing the diode current from 0 to 35A.

The user interface and the controller unit were developed previously for investigations of laser tissue interaction mechanisms. User interface and the controller unit control the output current. By controlling the output current and using the power vs current graph above, exposure time, power and the modulation type was set. Therefore the energy applied to the sample tissue was set.

Laser light was delivered to the tissue through a 400-µm silica optical fiber (Spindler–Hoyer, Göttingen, Germany). The tip of the fiber was not modified (i.e. flat ending). Output power was checked with the power meter frequently. Tip of the optical fiber was checked under a microscope (Motic, DMWB1-223 Digital Biological Microscope, Motic China Group Co. Ltd., Xiamen P.R.C, China) frequently and if any damage was observed, it was cut vertically with tungsten carbide knife.

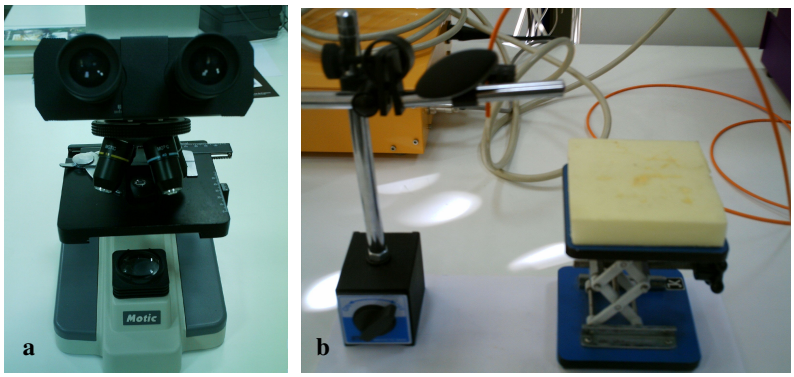

Figure 3.2 a. Motic Microscope. **b.** Experimental set for laser exposure.

The experimental set for laser exposure is shown on Figure 3.3.b. The fiber was fixed above the tissue sample at an angle of 90 degrees. The distance between the tip of the fiber and the surface of the sample tissue was set by adjusting the lever. A magnifier was used to check the flatness of the surface of the tissue.

For histological analyses Nüve Incubator (Nüve Sanayi Malzemeleri Imalat ve Tic. A.S., Istanbul), Leica RM2255 Microtome (Leica Microsystems, Nusloch, Germany) and Leica EG 1150 H Paraffin Embedding Station (Leica Microsystems, Nusloch, Germany) were used.

Figure 3.3 a. Incubator. **b.** Microtome. **c.** Paraffin embedding station.

For staining with H&E, Bio-Optica staining set was used.

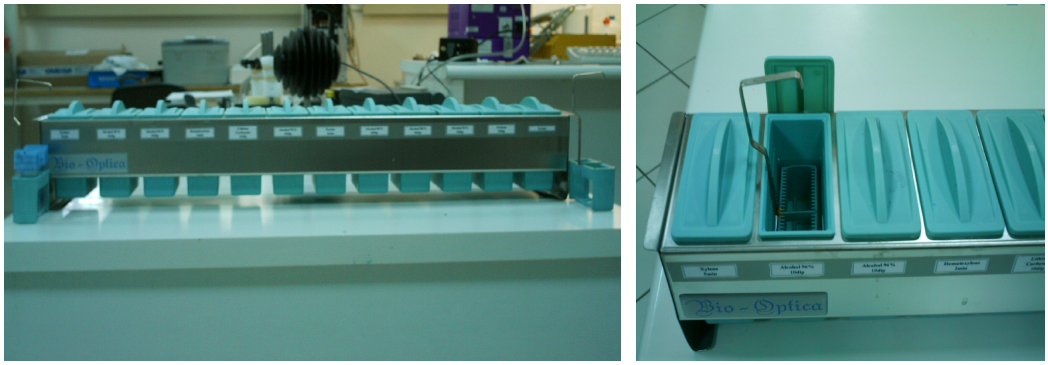

Figure 3.4 Bio-Optica staining set.

3.2 *in vitro* Study

The lamb tissues (liver, kidney and heart) were sliced into approximately 10 cm^3 pieces. During preliminary study was handled and the experiments were decided to be non-touch experiments. The tip of the optic fiber did not touch to the sample tissue and was approximately 250µm apart from the tissue. The beam spot size was 0.5 mm.

Three kinds of lamb tissue (liver, heart and kidney) and three different modes of laser (CW, 250 ms on/off and 50 ms on/off) were tested.

For continuous wave experiments there were two parameters; power and exposure time. For pulsed wave experiments, other parameters; number of cycles, and duration of on-off periods were added. Finally, energy calculated from these parameters was considered. For each parameter set (both CW and modulated) there were eight samples for statistical significance.

After the exposure, maximum diameter of the coagulated zone on the surface was measured by means of a micrometer. Then the sample tissue was cut in half carefully and the maximum depth was also measured with the micrometer. Before and after the cutting procedure photos of the tissue samples were taken and areas of thermal alteration (vaporization, carbonization and coagulation) were determined macroscopically. This procedure continued by increasing the given energy by means of changing the exposure time until carbonization was observed. The experiment was finished when carbonization was observed.

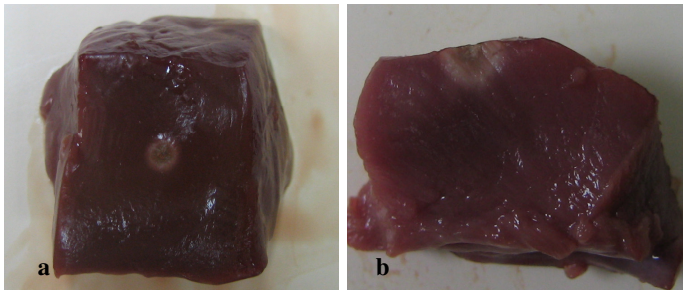

Figure 3.5 Example for a coagulated tissue. **a.** Surface **b.** Inside.

The average value and the standard deviation of each set (each set has eight samples that were irradiated under same parameters) were calculated. Optimum parameters for each modulation type and for each tissue were chosen.

3.3 Histology

Parameters found to be optimum were evaluated in a new set of experiment for histological analysis. After the exposure tissues were fixed in paraformaldehyde (PFA) solution for a day.

Table 3.1
Contents of the PBS Formalin Solution

Preparation of PBS Formalin	
Di-Sodium Hydrogen Phosphate	14,8gr
Sodium Di-Hydrogen Phosphate	4,3gr
Sodium Chloride	72gr
Distilled Water	10 liters
Formaldehyde	1 liter

After PBS Formalin fixation process continued as follows. The samples were immersed in multiple baths of progressively more concentrated ethanol to dehydrate the tissue, followed by a clearing agent, xylene, and finally hot melted paraffin wax. During this process, paraffin wax repleaced the water. Soft, moist tissues were turned into a hard paraffin block.

Table 3.2
The dehydration process

Dehydration		
1	96% Alcohol	15 minutes
2	100% Alcohol	30 minutes
3	100% Alcohol	30 minutes
4	Xylene	30 minutes
5	Xylene	30 minutes
6	Paraffin	30 minutes
7	Paraffin	30 minutes

Dehydrated tissue blocks were then placed in cassettes containing more molten paraffin wax (embedded) and allowed to cool and harden.

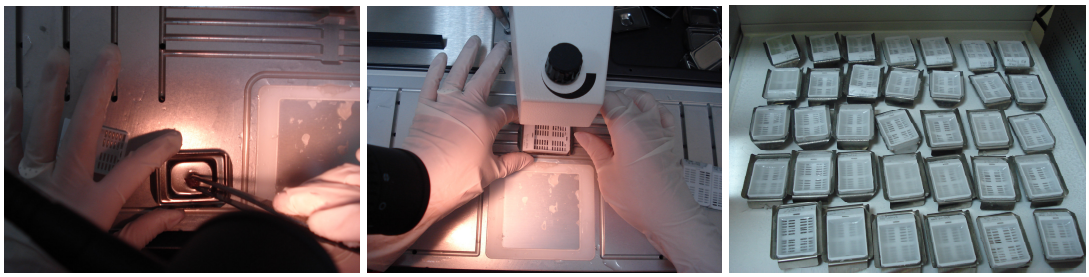

Figure 3.6 The sample tissue cassettes were filled with melted paraffin and frozen.

The next procedure after embedding the tissue samples in paraffin filled cassettes, was sectioning. By using the microtome five micrometer slices were taken on the slides.

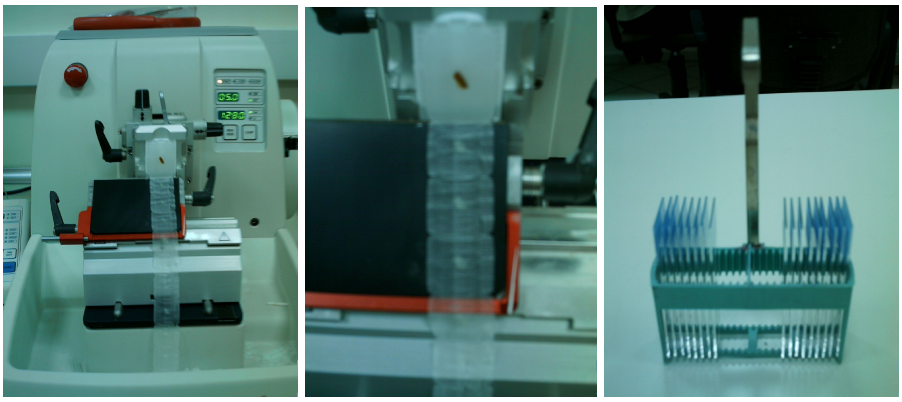

Figure 3.7 Sample tissues were sliced with microtome and taken on slides for staining.

To see the tissue under a microscope, the sections were stained with one or more pigments. This was done to give contrast to the tissue being examined, as without staining it was very difficult to see differences in cell morphology. Hematoxylin and eosin (H&E) are the most commonly used stains in histology and histopathology. Hematoxylin colors nuclei blue, eosin colors the cytoplasm pink. For staining, the following procedure was performed.

Table 3.3
The staining procedure.

Staining		
1	Melt the paraffin on the slide	1 hour
2	Xylene	5 minutes
3	96% Alcohol	10 dip
4	96% Alcohol	10 dip
5	Wash with tap water	
6	Hematoxylin	2 minutes
7	Wash with tap water	
8	Lithium Carbonate	10 dip
9	Wash with tap water	
10	96% Alcohol	10 dip
11	Eosine	2 minutes
12	96% Alcohol	10 dip
13	96% Alcohol	10 dip
14	96% Alcohol	10 dip
15	Acetone	10 dip
16	Dry	
17	Xylene	1 Dip
18	Close the slide with entellan	

At the end of the staining procedure the slides were examined and photographed under microscope.

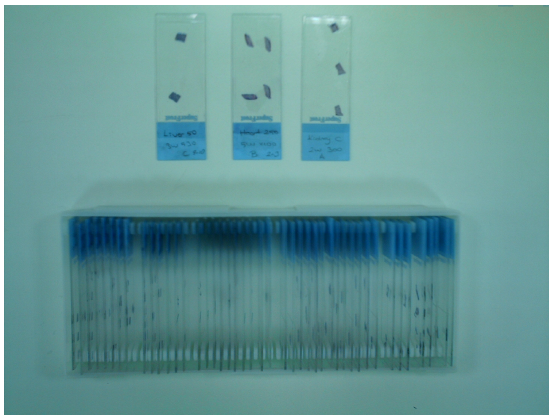

Figure 3.8 The tissue slices were stained and fixed on slides.

4. RESULTS

With the onset of carbonization the optical properties of the tissue, the absorption and the scattering coefficients of the tissue are changed. Therefore the delivered laser energy may cause unexpected thermal changes. Carbonization does not only prolong the healing process but also change the laser operation conditions. This is another reason why carbonization of target tissue must be avoided. So the irradiation process continued by increasing the delivered energy until carbonization was observed, that is maximum energy density for a specific power density to coagulate the tissue without carbonization was achieved.

The results are classified according to tissue type. For each tissue the order of the irradiation types will be continuous mode, 250 ms on/off modulated wave and finally 50 ms on/off modulated wave. All power densities for an irradiation mode were shown on a graph for comparison. The graphs of each power density were given in appendices. After the results of each tissue the histological sections of proposed best doses were shown for that tissue.

4.1 Liver

4.1.1 Continuous Mode

For continuous mode, maximum energy density that could be applied to lamb liver was 81 J/mm^2 and maximum irradiance was 20.4 W/mm^2. Above this level carbonization was observed instantaneously. The maximum average diameter of the coagulated zone on the surface was 2,65 mm and the depth was 1,19 mm. Best proposed dose for liver under continuous irradiation was 15.3 W/mm^2, 76 J/mm^2.

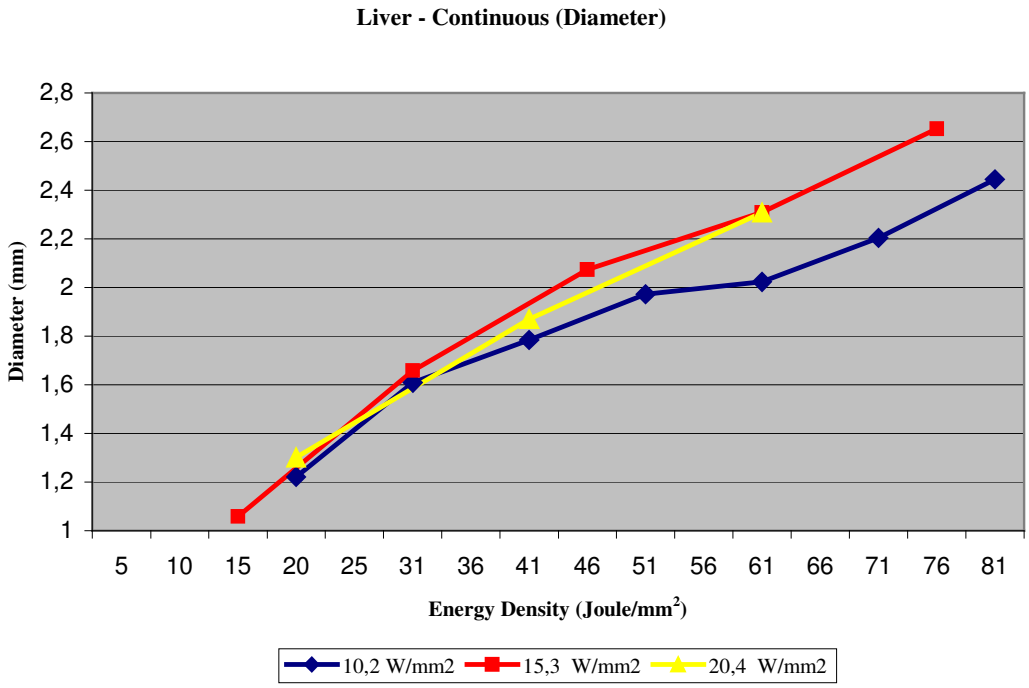

Figure 4.1 Applied power density, energy density and the corresponding lesion diameters are shown on the graph.

For continuous mode all power densities those could be applied to the lamb liver were given in Figure 4.1. Each line on the graph represented the curve of a power density. The resulting diameters on the surface were almost equal up to 40 J/mm^2. As the energy increased by increasing the irradiation duration, 10.2 W/mm^2 curve separated from the other. The reason of this difference was mostly because the heat accumulation by 15.3 W/mm^2 and 20.4 W/mm^2 increased the temperature of the tissue faster than 10.2 W/mm^2 power density did. Therefore, the resulting lesion was larger. Generally the area of the coagulated zone at a fixed energy density enlarges as the power increases but in this experiment since the energy density was very low (81 J/mm^2 maximum) it could not be observed clearly. Since coagulation was observed at 20.4 W/mm^2 61 J/mm^2, the energy could not be increased. 15.3 W/mm^2 76 J/mm^2 was best parameter for maximum diameter.

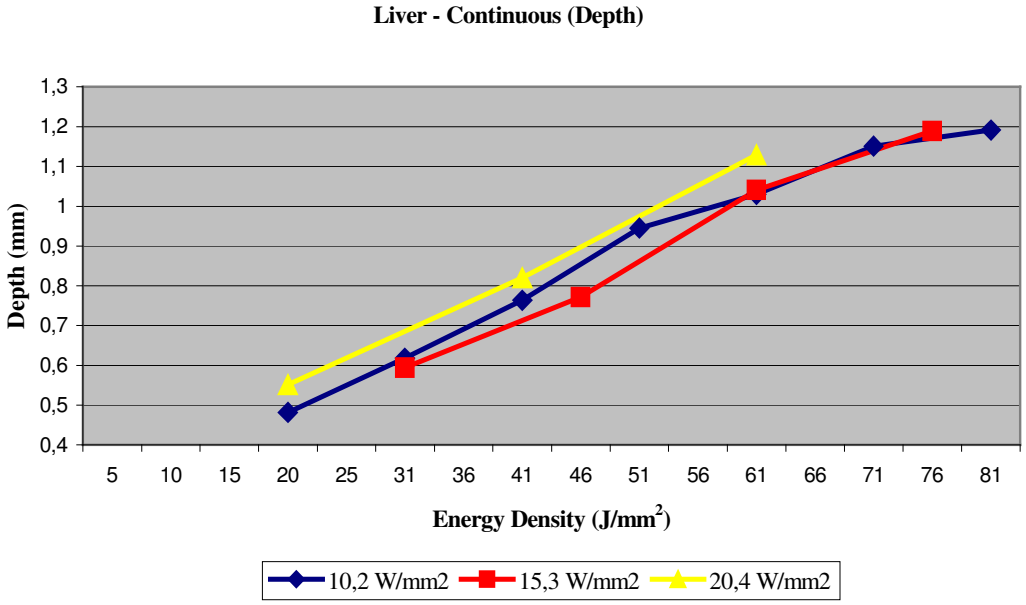

Figure 4.2 Applied power density, energy density and the corresponding lesion diameters.

Since the energy density of the liver tissue was very low in this experiment the results were very close, but the 20.4 W/mm^2 line showed that if the power was increased at a fixed energy level the resulting lesion depth increased also. Although the maximum power density was 20.4 W/mm^2, the maximum depth was achieved with 15.3 W/mm^2 since carbonization did not allow increasing the energy above 61 J/mm^2 for 20.4 W/mm^2. 15.3 W/mm^2, 76 J/mm^2 was the best parameter for maximum coagulation.

4.1.2 250ms ON/OFF Modulated Wave

For 250 ms on/off modulated wave, maximum energy density was 382 J/mm^2 (10.2 W/mm^2 150 cycles) and maximum power density was 30.5 W/mm^2. Above this level carbonization was observed instantaneously. Maximum average diameter of the coagulated zone on the surface was 3.80 mm and the depth was 1.86 mm. Compared to continuous mode, energy density increased to 382 J/mm^2 from 76 J/mm^2, power density increased to 30.5 W/mm^2 from 20.4 W/mm^2, diameter increased to 3.80 mm from 2.65 mm and the depth increased to 1.86 mm from 1.19 mm. Best proposed dose for liver under 250 ms on/off modulated wave irradiation was 20.4 W/mm^2 382 J/mm^2.

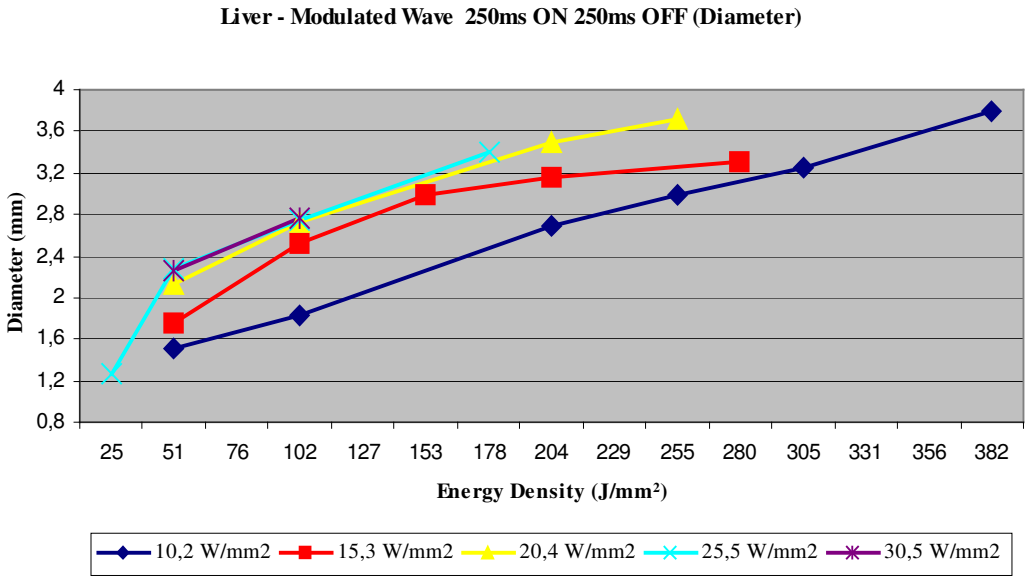

Figure 4.3 Applied power density, energy density and the corresponding lesion diameters.

Changing the mode of operation from continuous to modulated wave increased maximum energy density and maximum power density. Maximum lesion diameter achieved by 250 ms on/off modulated wave was 3.80 mm with a standard deviation of 0.11. At a fixed energy density, the diameter of the coagulation zone increased by increasing the power density. For example; the diameter of the coagulated zone at 102 J/mm^2 for 10.2 W/mm^2 was 1.83 mm whereas it was 2.76 mm for 30.5 W/mm^2.

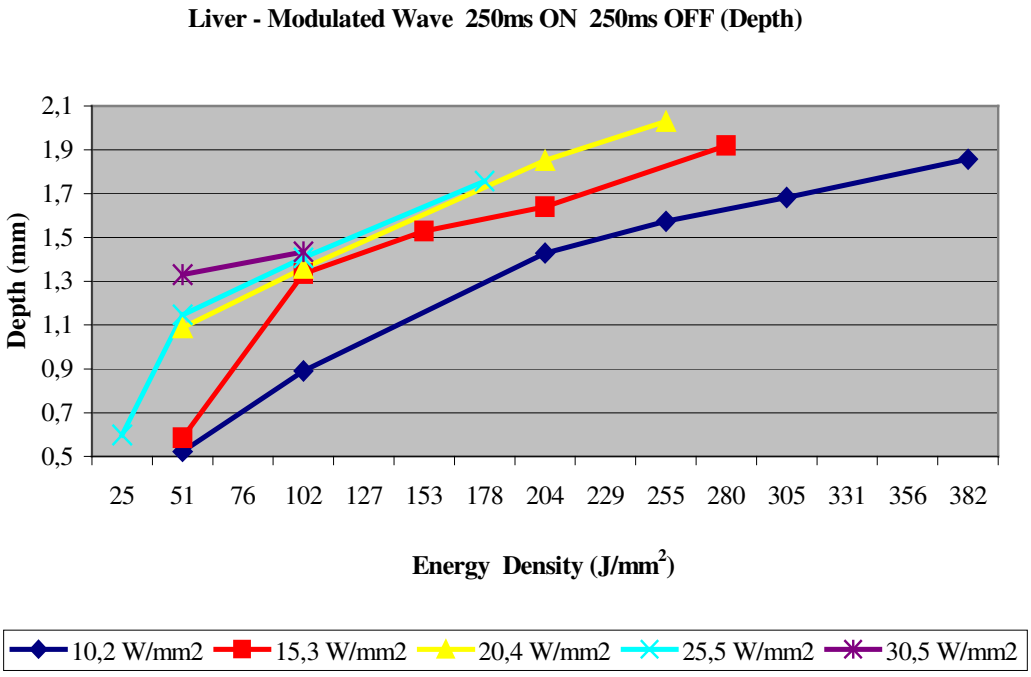

Figure 4.4 Applied power density, energy density and the corresponding lesion diameters.

The depth-energy density graph of liver 250 ms on/off modulation type was given in Figure 4.4. It was mentioned before that for this modulation type maximum 30.5 W/mm^2 could be applied to the tissue, above this level carbonization occurred instantaneously. Maximum power density was not enough to coagulate the maximum area because of the low carbonization threshold compared to a low power density, high energy density was needed for larger coagulations. In Figure 4.4 if 30.5 W/mm^2 and 10.2 W/mm^2 were compared, for 30.5 W/mm^2 maximum energy delivered to the tissue without carbonization was 102 J/mm^2, on the other hand the maximum energy delivered to the tissue for 10.2 W/mm^2 was 382 J/mm^2. 30.5 W/mm^2 delivered the energy three times faster compared to 10.2 W/mm^2 but in contrast the quantity of the energy density of 10.2 W/mm^2 was almost four times of 30.5 W/mm^2. Finally the maximum depth of the coagulated zone was larger for 10.2 W/mm^2.

The maximum depth achieved was 2.03 mm with a standard deviation of 0.09 mm with 20.4 W/mm^2 irradiance. The second best one was with 15.3 W/mm^2 irradiance, which

was 1.92 mm with a standard deviation of 0.07 mm. And the third one was 1.86 mm with a standard deviation of 0.18 mm under 10.2 W/mm^2.

4.1.3 50 ms ON/OFF Modulated Wave

The maximum power density that can be applied without carbonization increased up to 46.8 W/mm^2 as the on/off periods decreased to 50 ms. Shorter durations decreased the heat accumulation in the tissue, the tissue had more time for relaxation and finally maximum power increased. Beside maximum power, maximum energy was also increased. The results of 15.3 W/mm^2, 20.4 W/mm^2, 25.5 W/mm^2 and 30.5 W/mm^2 were very close between 3,90 mm - 4,00 mm. High power density (35.6 W/mm^2 – 50.9 W/mm^2) led carbonization rapidly compared to low power density (10.2 W/mm^2 – 30.5 W/mm^2). Best proposed dose was 15.3 W/mm^2 407 J/mm^2.

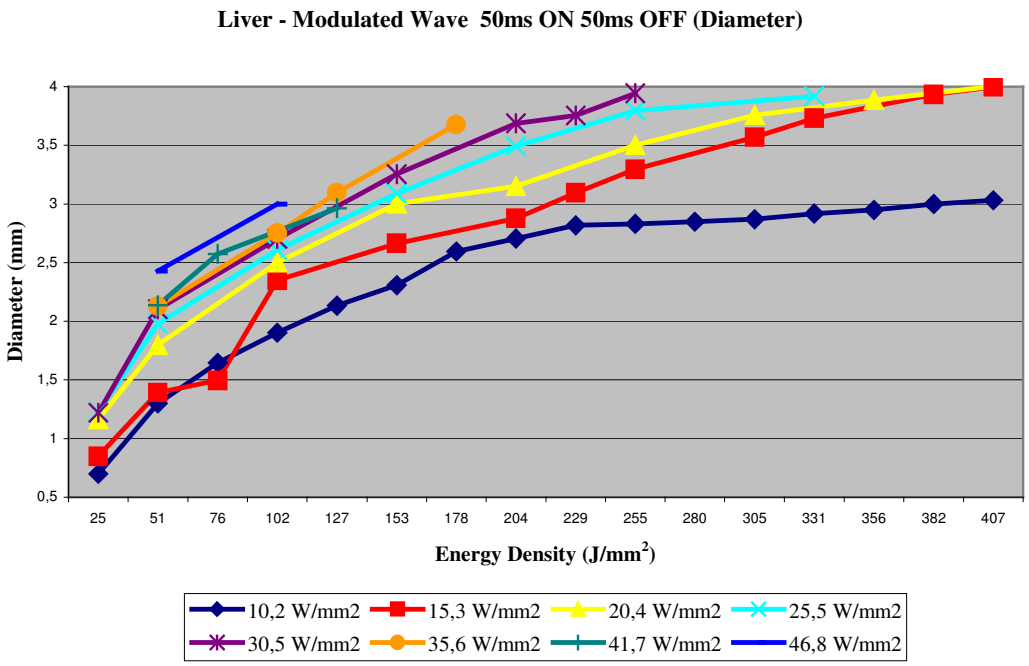

Figure 4.5 Applied power density, energy density and the corresponding lesion diameters.

In Figure 4.5, if the lines were grouped 10.2 W/mm^2 and 46.8 W/mm^2 had different paths, 15.3 W/mm^2, 20.4 W/mm^2 and 25.5 W/mm^2 had similar paths and finally 30.5 W/mm^2, 35.6 W/mm^2 and 41.7 W/mm^2 showed very similar characteristics. 10.2 W/mm^2 turned to be parallel to x-axis after 204 J/mm^2 and the diameter stayed almost

constant while the energy was increased 100%. This threshold was 356 J/mm^2 for 15.3 W/mm^2 and 20.4 W/mm^2, 255 J/mm^2 for 25.5 W/mm^2. There may be two reasons for this threshold. The first one is, since the optical properties of the tissue had changed, the scattering coefficient of the tissue increased and the absorption coefficient decreased, light cannot be absorbed by water, heat generation decays and temperature does not reach the threshold for coagulation. The second one is, since the tissue loses water, it shrinks down, the distance between the fixed laser tip and surface of the tissue increases and finally focal point enlarges. The result of this is a decrease in the energy density of the targeted area that leads to temperature decrease.

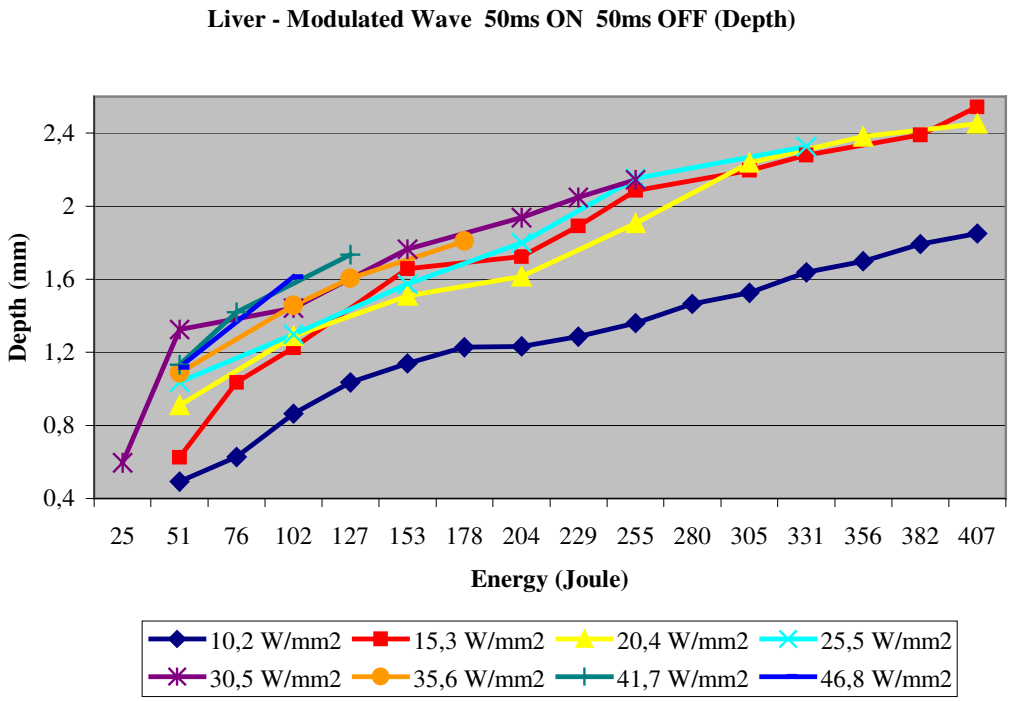

Figure 4.6 Applied power density, energy density and the corresponding lesion diameters.

Low power density led the disadvantage of decrease in diameter and depth both. On the other hand, since the temperature increase was slow for 10.2 W/mm^2, the probability of carbonization occurrence and to damage the adjacent tissue decreased.

The maximum depth that could be reached was around 2.5 mm that was achieved with 15.3 W/mm^2, 20.4 W/mm^2 and 25.5 W/mm^2. The intersection at the maximum point

was a result of the change in optical properties. Power densities between 15.3 – 30.5 W/mm^2 may be used according to the desired operation time.

Above 30.5 W/mm^2, the curves were almost linear. It was because of the high power density of the irradiation. Below 35.5 W/mm^2, tissue shrank indicating the water evaporation but at high power, tissue did not shrink, focal point size and the power density stayed constant. The temperature increase was so rapid that tissue was coagulated before the evaporation of water.

The best dose for 50 ms on/off modulated wave was 15.3 W/mm^2 407 J/mm^2. Diameter was 4.00 mm with a standard deviation of 0.15 mm and depth was 2.54 mm with a standard deviation of 0.06 mm.

4.1.4 Histology

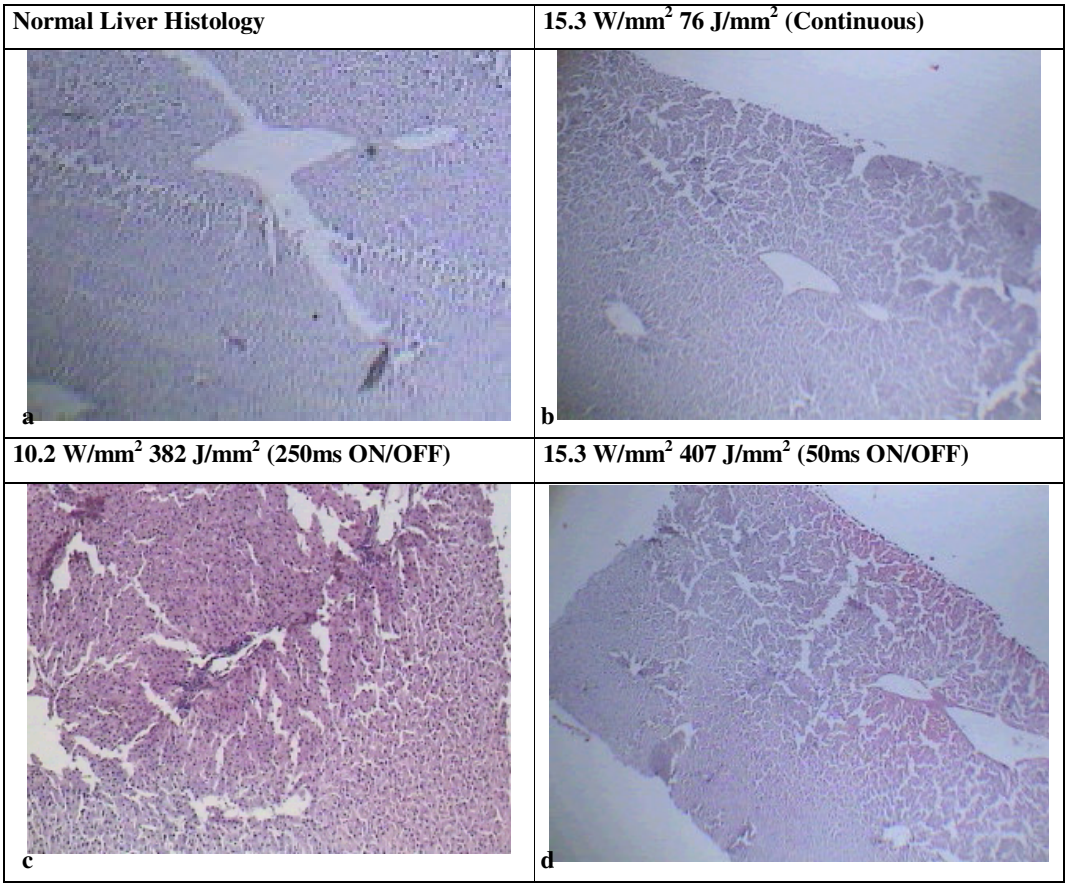

Figure 4.7 Histological sections for the chosen parameters for liver. **a.** Normal liver histology. **b.** Histology of liver irradiated with continuous wave. **c.** Histology of liver irradiated with 250ms on/off modulated wave. **d.** Histology of liver irradiated with 50ms on/off modulated wave.

The results of liver histology showed that the thermal alteration did not differ with the modulation type. Results were same for continuous wave and the modulated wave. The diameter and the depth of the coagulated zones were larger for modulated irradiation. Thermal alteration of liver was observed by histological analyses.

4.2 Heart

4.2.1 Continuous Mode

The maximum power density applied without carbonization was increased to 30.5 W/mm^2 compared to liver (20.4 W/mm^2). Maximum energy density increased to 611 J/mm^2, it was 81 J/mm^2 for liver.

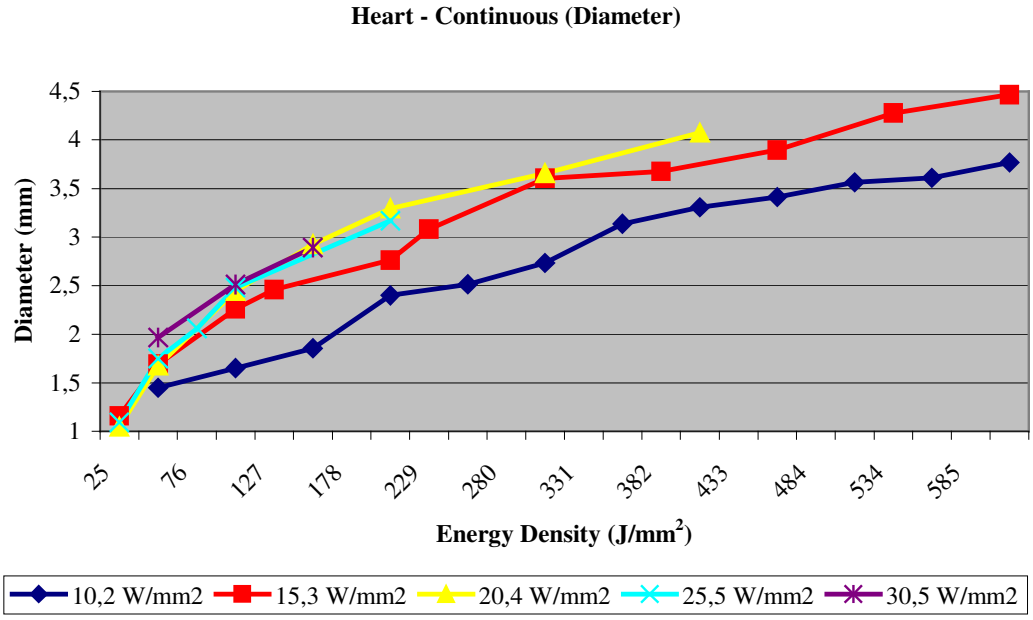

Figure 4.8 Applied power density, energy density and the corresponding lesion diameters.

In Figure 4.8 maximum energy was 611 J/mm^2 for 15.3 W/mm^2, which corresponded to a 40 second continuous irradiation at 3 W output power of laser. At the end of the experiment the best power parameter for continuous irradiation was found 15.3 W/mm^2 that achieved a coagulated zone of diameter 4.47 mm. At the same energy level (611 J/mm^2) 10.2 W/mm^2 coagulated a zone that's diameter was 0.8 mm smaller than 15.3 W/mm^2. One can enlarge the coagulated area by increasing power density while decreasing the time of irradiation. There are to alternatives to increase the power density, by decreasing the beam spot size or by increasing the output power of the laser.

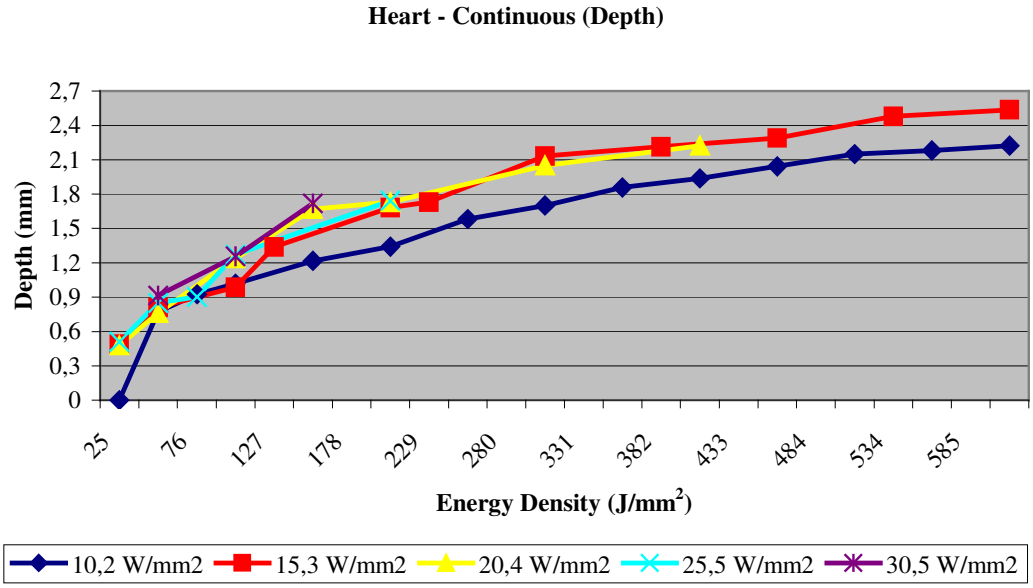

Figure 4.9 Applied power density, energy density and the corresponding lesion diameters.

At some threshold value the depth of the coagulated zone stayed almost constant. In Figure 4.9, above 500 J/mm^2 the change of depth was not significant. The results were almost equal above 10.2 W/mm^2 until 200 J/mm^2. The best proposed dose for coagulation of heart under continuous irradiation was 15.3 W/mm^2 611 J/mm^2. The diameter of the coagulated zone was 4.47 mm with a standard deviation of 0.10 mm and the depth was 2.54 mm with a standard deviation of 0.13 mm.

4.2.2 250ms ON/OFF Modulated Wave

Maximum energy delivered to tissue was 1909 J/mm^2 (15.3 W/mm^2), it was 611 J/mm^2 for continuous mode. Because of the 5 minutes time limit, 10.2 W/mm^2 irradiation was stopped at 1909 J/mm^2. Normally, time limit for 10.2 W/mm^2 corresponded to 1527 J/mm^2 but to show that the results after 5 minutes were not significant; the energy density was increased to 1909 J/mm^2.

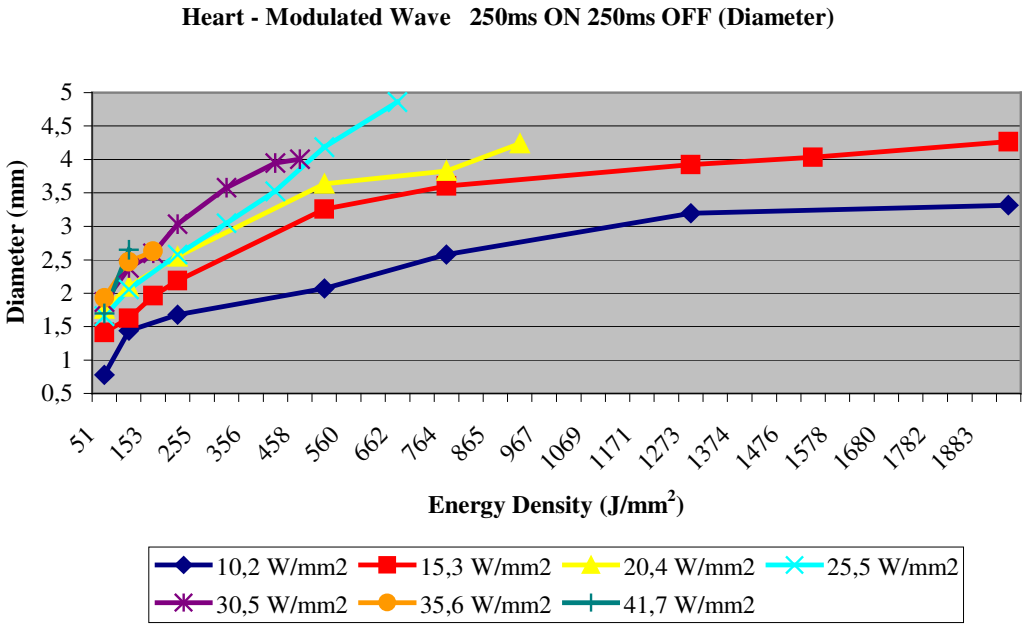

Figure 4.10 Applied power density, energy density and the corresponding lesion diameters.

The comparison of continuous to 250 ms on/off results was similar to liver. If the mode of operation was changed, the maximum power density without carbonization and the maximum energy density increased. As the mode of operation changed to modulated wave, maximum power density increased to 41.7 W/mm^2 from 30.5 W/mm^2 and maximum energy delivered to the tissue increased from 153 J/mm^2 to 458 J/mm^2. The maximum diameter achieved with 30.5 W/mm^2 under continuous irradiation was 2.90 mm and the depth was 1.70 mm. On the other hand maximum diameter for 250 ms on/off modulated wave was 4.00 mm and the depth was 2.10 mm. Maximum diameter was achieved by 25.5 W/mm^2 and the maximum energy delivered to the tissue was 636 J/mm^2. 10.2 W/mm^2 experiment stopped at 1909 J/mm^2 since the time limit exceeded. The limit was 5 minutes for total time, that is the sum of on and off periods.

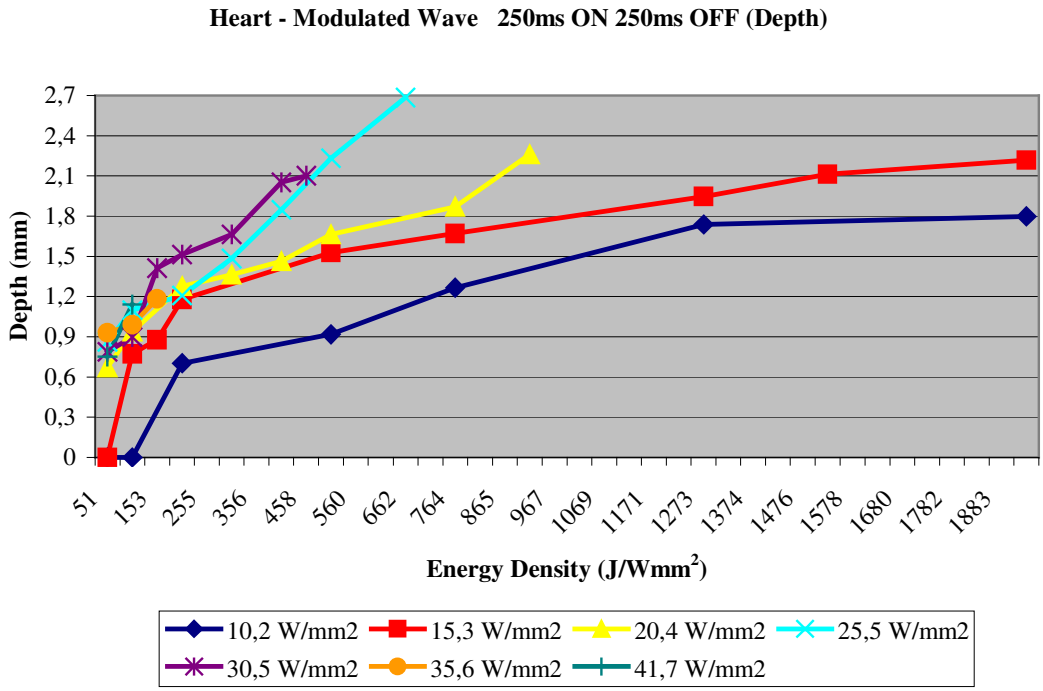

Figure 4.11 Applied power density, energy density and the corresponding lesion diameters.

For 10.2 W/mm^2, results at 1273 J/mm^2 and 1909 J/mm^2 were almost equal and the p value of the T-test was 0.07, which is larger than 0.05. Thus the results were not significant although the energy density was increased by 50%. 15.3 W/mm^2 and 20.4 W/mm^2 had equal maximums but the total operation time was 90 seconds for 20.4 W/mm^2 but 250 seconds for 15.3 W/mm^2. The total time may be important at some circumstances. 25.5 W/mm^2 and 20.4 W/mm^2 were the best two parameters for penetration in heart.

The best proposed dose for coagulation of heart with 250 ms on/off modulated wave was 25.5 W/mm^2 636 J/mm^2. The diameter of the coagulated zone was 4.86 mm with a standard deviation of 0.13 mm and the depth was 2.68 mm with a standard deviation of 0.07 mm.

4.2.3 50ms ON/OFF Modulated Wave

Since on/off periods decreased to 50 ms, heat accumulation in the tissue decreased, total irradiation time and energy delivered to the tissue increased. Extra experiments were also done to see the characteristics after five minutes, the results were not significant.

Maximum diameters were achieved with 20.4 W/mm^2 and 25.5 W/mm^2. As power increased, the diameter of the coagulated zone decreased since the energy delivered to the tissue decreased. Above 30.5 W/mm^2, the characteristics were similar and the resulting diameters for a given energy level were not significant.

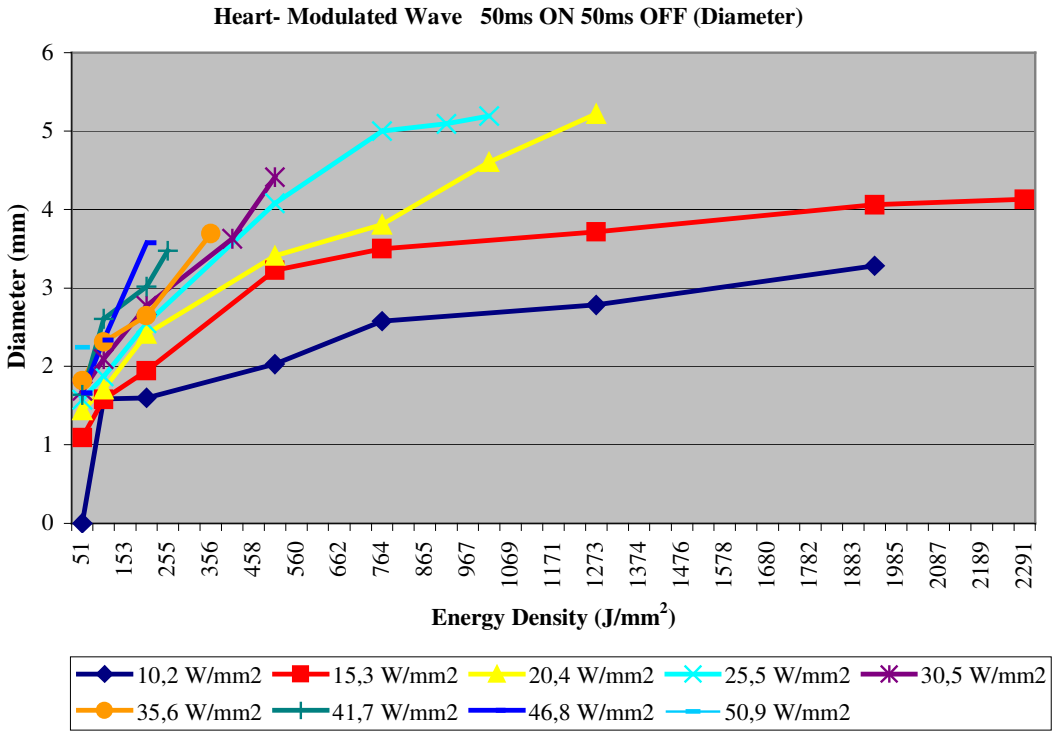

Figure 4.12 Applied power density, energy density and the corresponding lesion diameters.

Similar to the diameter results the best parameters for maximum depth were 20.4 W/mm^2 and 25.5 W/mm^2. The results were around 3 mm, which was the maximum depth achieved on heart. It was deeper than the coagulation depth of continuous irradiation and also 250ms on/off modulated wave. In Figure 4.13, the depth increased when the

power increased at a specific energy level. For example at 509 J/mm^2, 15.3 W/mm^2 depth was 1.55 mm, 20.4 W/mm^2 depth was 1.75 mm and 25.5 W/mm^2 depth was 2.27 mm.

Above 25.5 W/mm^2, before carbonization, bubble formation was observed. The surface of the tissue was strained, a small bubble was observed then the bubble blew up. During this bubble formation most of the energy dissipated and the enlargement of the coagulated zone had stopped. Therefore the power increase above 25.5 W/mm^2 did not contribute to coagulation very much.

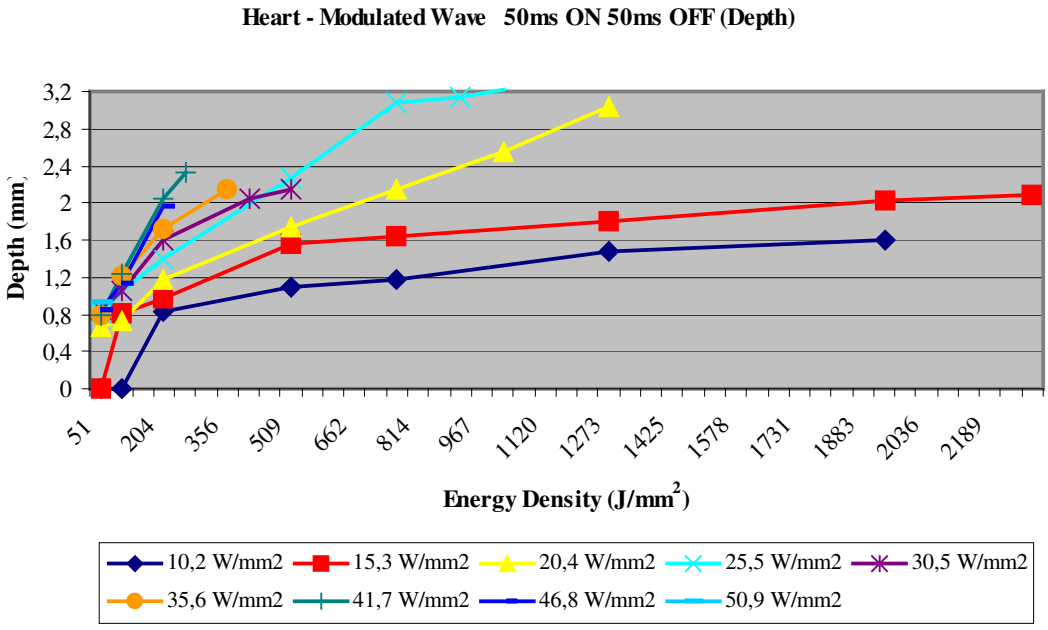

Fig 4.13 Applied power density, energy density and the corresponding lesion diameters.

The best proposed dose for coagulation of heart with 50 ms on/off modulated wave was 25.5 W/mm^2 1018 J/mm^2 The diameter of the coagulated zone was 5.19 mm with a standard deviation of 0.11 mm and the depth was 3.22 mm with a standard deviation of 0.12 mm.

4.2.4 Histology

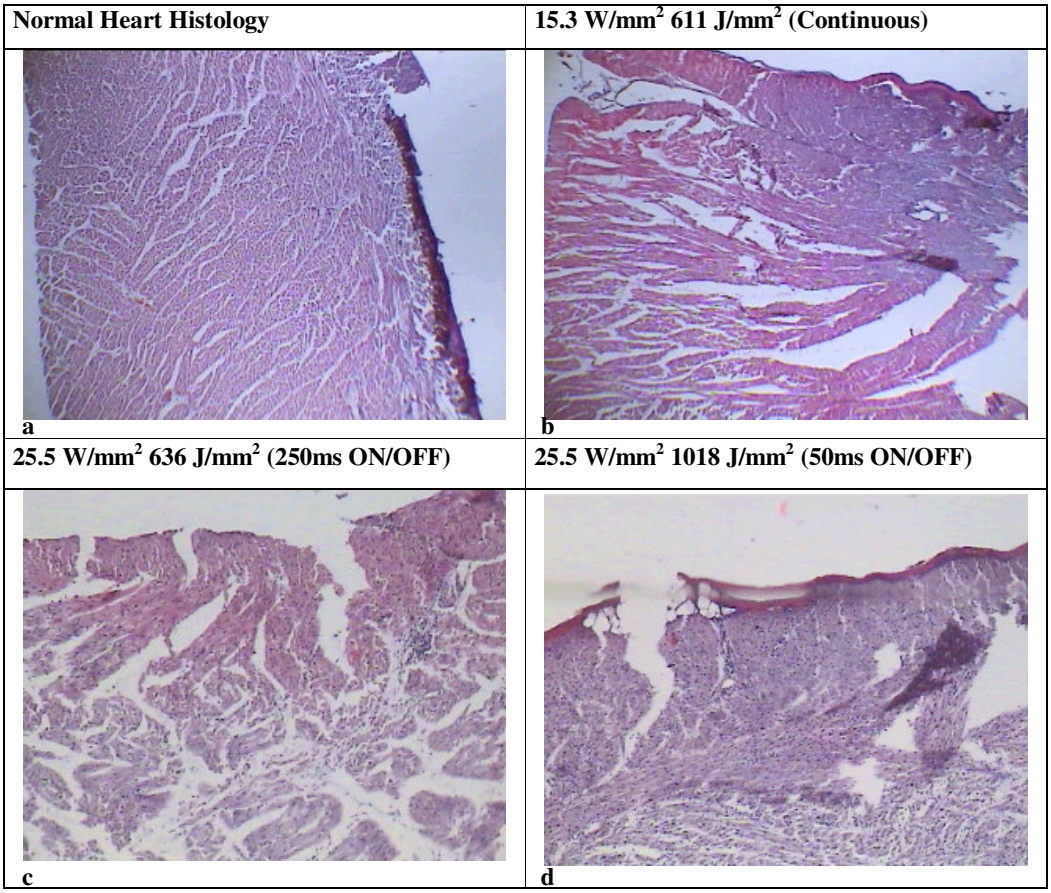

Figure 4.14 Histological sections for the chosen parameters for heart. **a.** Normal heart histology. **b.** Histology of heart irradiated with continuous wave. **c.** Histology of heart irradiated with 250ms on/off modulated wave. **d.** Histology of heart irradiated with 50ms on/off modulated wave.

Thermal alteration of heart was observed by histological analyses. The results were same for each modulation type (continuous, 250ms on/off and 50 ms on/off). The junction between endocardium and the myocardium were lost and the structure was changed towards the surface.

4.3 Kidney

4.3.1 Continuous Mode

The maximum power applied without carbonization was increased to 35.6 W/mm^2 compared to liver (20.4 W/mm^2) and heart (30.5 W/mm^2). Maximum energy delivered increased to 3054 J/mm^2, it was 81 J/mm^2 for liver and 611 J/mm^2 for heart.

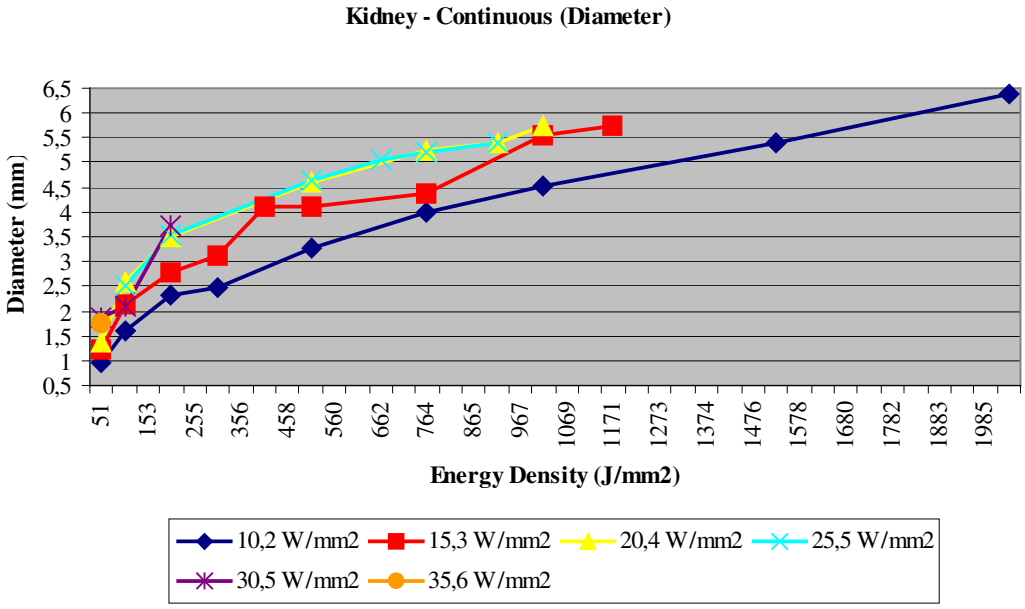

Figure 4.15 Applied power density, energy density and the corresponding lesion diameters.

For 10.2 W/mm^2 irradiation maximum energy delivered to the tissue was 3054 J/mm^2 and the resulting diameter was 6.81 mm, for 15.3 W/mm^2 it was 5.76 mm. The paths of 20.4 W/mm^2 and 25.5 W/mm^2 graphics collided with each other. Carbonization threshold decreases dramatically above 25.5 W/mm^2, it was 204 J/mm^2 for 30.5 W/mm^2 and 51 J/mm^2 for 35.6 W/mm^2. The results were linear for 30.5 W/mm^2 and 35.6 W/mm^2 because of the rapid elevation of temperature and coagulation of the tissue before evaporation of water.

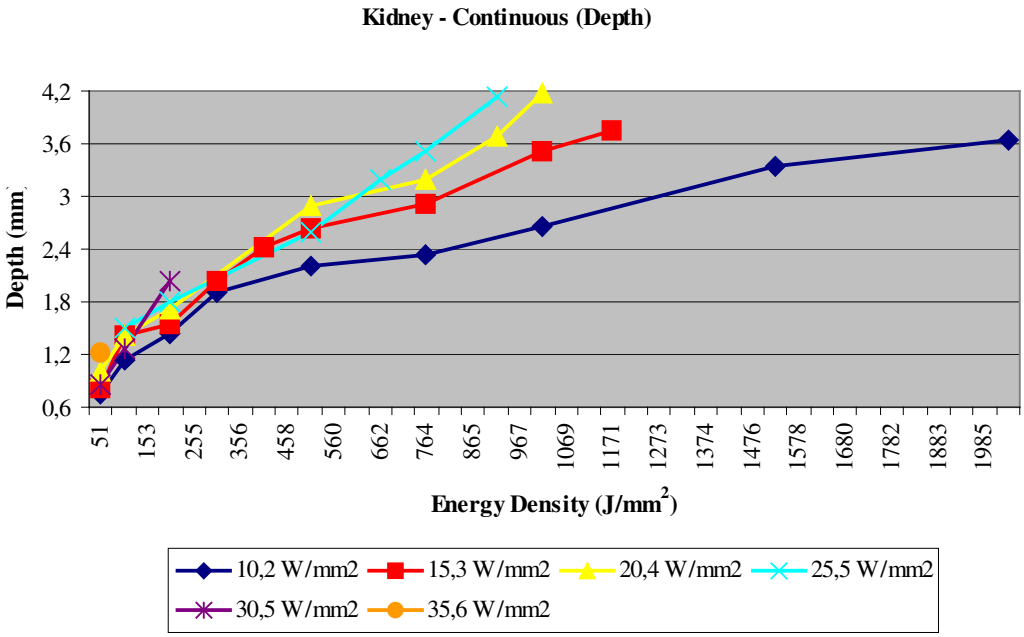

Figure 4.16 Applied power density, energy density and the corresponding lesion diameters.

Below 30.5 W/mm^2 all maximum diameters were above 3.6 mm. 20.4 W/mm^2 and 25.5 W/mm^2 results were 4.17 mm and 4.13 mm respectively. Compared to 15.3 W/mm^2, 20.4 W/mm^2 and 25.5 W/mm^2, which had similar characteristics, the energy density achieved by 10.2 W/mm^2 is 200% more.

For continuous irradiation of kidney maximum diameter, and depth were achieved by 10.2 W/mm^2, which had the minimum output power (2 W). The maximum energy delivered to the tissue was around 1000 J/mm^2 for 15.3 W/mm^2 - 25.5 W/mm^2 and the diameter and depth characteristics were very similar. As power increased the energy delivered to the tissue decreases, above 25.5 W/mm^2 the diameter and depth measurement results dropped dramatically since the decay of the energy delivery.

The best proposed dose for coagulation of kidney with continuous wave was 10.2 W/mm^2 600 J/mm^2. The diameter of the coagulated zone was 6.81 mm with a standard deviation of 0.05 mm and the depth was 4.38 mm with a standard deviation of 0.04 mm.

4.3.2 250ms ON/OFF Modulated Wave

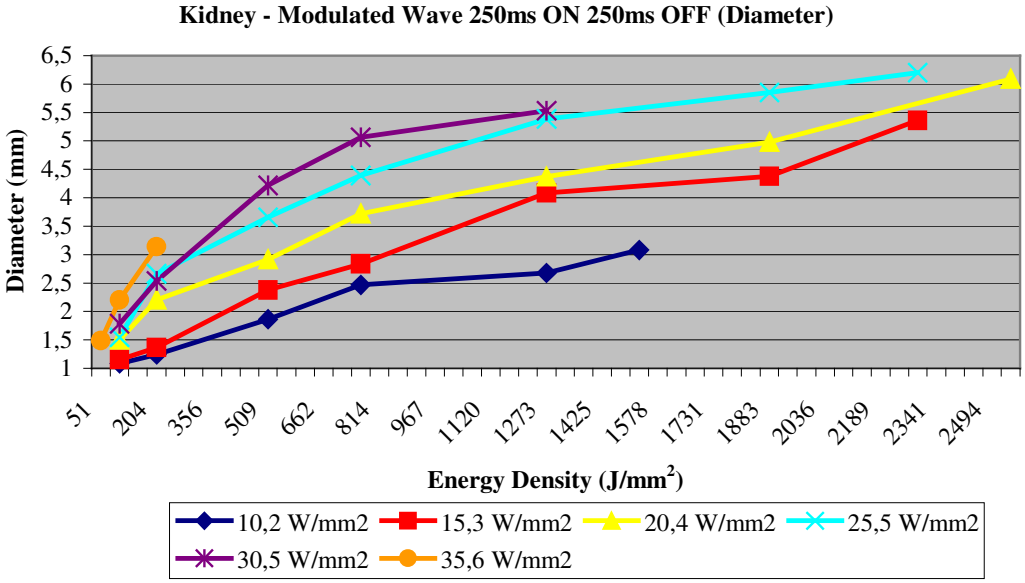

Figure 4.17 Applied power density, energy density and the corresponding lesion diameters.

In Figure 4.17, 10.2 W/mm^2 and 15.3 W/mm^2 irradiations were stopped after 5 minutes. The characteristics of irradiance curves were similar, slope decreased as energy density increased. At a fixed energy density, increasing the power density increased diameter. On the other hand, increasing the power density, decreased the carbonization threshold. For example; carbonization threshold for 20.4 W/m^2 was 2545 J/mm^2, whereas it was 204 J/mm^2 for 35.6 W/mm^2. Maximum energy density was 2545 W/mm^2 for 20.4 W/mm^2. Maximum diameter was achieved by 25.5 W/mm^2 (6.20 mm).

35.6 W/mm^2 and 30.5 W/mm^2 (until 500 J/mm^2) had linear results. Since the power density was high, heat generation inside the tissue was rapid. Before evaporation of water temperature increases rapidly and tissue was coagulated. Since water did not evaporate, convection of heat did not occur.

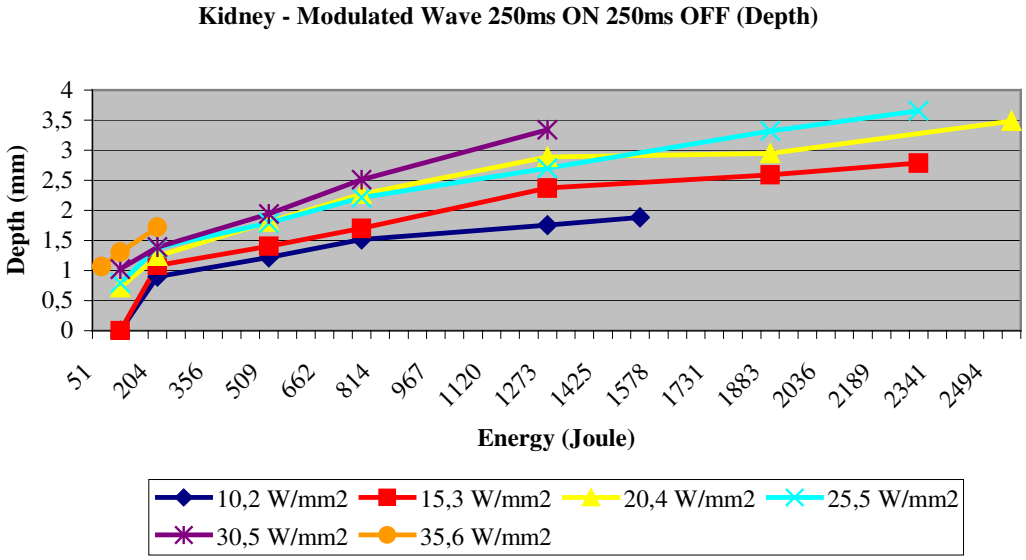

Figure 4.18 Applied power density, energy density and the corresponding lesion diameters.

The depth-energy density graph of kidney 250 ms on/off modulation type was given in Figure 4.18. It was mentioned before that for this modulation type maximum 35.6 W/mm^2 could be applied to the tissue, above this level carbonization occurred instantaneously. Maximum depth was achieved by 25.5 W/mm^2 (3.66 mm). Linear parts of the curves were more clear in Figure 4.18. Up to 1200 J/mm^2 the depth increased linearly. The penetration depth of 980 nm diode laser was around 2 mm, but heat conduction and anisotropic scattering (*g* scattering) together increased the temperature of the deep inside. By heat conduction, the generated heat in the upper parts of tissue was conducted deeper, increasing the temperature. By *g* scattering light was transmitted to deeper parts of the tissue, absorbed by water and turned into heat energy. Both mechanisms increased the temperature deep inside the tissue and led to coagulation of the tissue.

The best proposed dose for coagulation of kidney with 250 ms on/off modulated wave was 25.5 W/mm^2 2291 J/mm^2 . The diameter of the coagulated zone was 6.20 mm with a standard deviation of 0.08 mm and the depth was 3.66 mm with a standard deviation of 0.08 mm.

4.3.3 50ms ON/OFF Modulated Wave

10.2 W/mm^2 and 15.3 W/mm^2 irradiations were cut at 1527 W/mm^2 and 2291 J/mm^2 respectively because of the 5 minutes time limit. Maximum energy delivery at 20.4 W/mm^2 without carbonization was 3054 W/mm^2, which was also equal to the time limit 5 minutes. Maximum diameter achieved without carbonization was around 6mm for all power densities from 20.4 W/mm^2 to 35.6 W/mm^2. The most important point is power increase results in energy decrease for a fixed diameter. But it is also important that lower power levels are safer for the adjacent tissue. On Table 4.1, the power increase caused the diameter and the depth of the coagulated zone to increase.

Table 4.1
Resulting diameters and depths for different power levels at 764 J/mm^2.

Power Density	**10.2 W/mm^2**	**15.3 W/mm^2**	**20.4 W/mm^2**	**25.5 W/mm^2**	**30.5 W/mm^2**	**35.6 W/mm^2**
Diameter (mm)	2,03	2,48	3,41	4,17	4,63	4,76
Depth (mm)	1,14	2,34	2,43	2,88	3,22	3,58

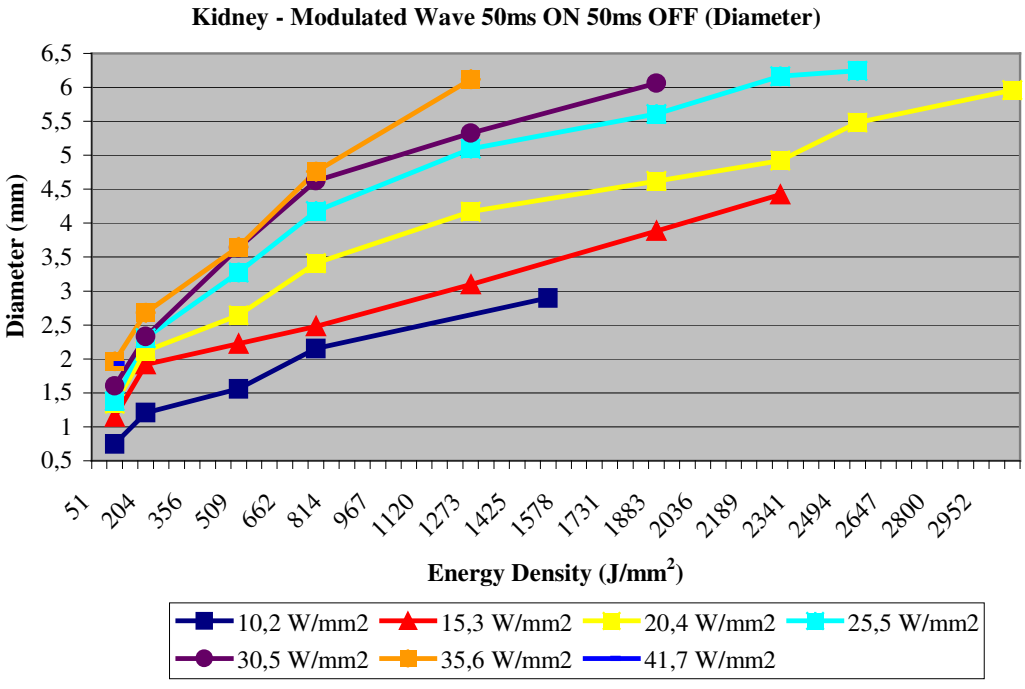

Figure 4.19 Applied power density, energy density and the corresponding lesion diameters.

.

In Figure 4.20, 10.2 W/mm^2 was not efficient when compared to 15.3 W/mm^2 and 20.4 W/mm^2. Lines of 15.3 W/mm^2 and 20.4 W/mm^2 power densities as well as lines of 25.5 W/mm^2, 30.5 W/mm^2, and 35.6 W/mm^2 power densities showed similar characteristics except the carbonization threshold which decreases as the power increases. In this experiment maximum depth was achieved by 30.5 W/mm^2 (4.36 mm). Also, the depth for 25.5 W/mm^2 was over 4 mm as well. In addition, the other high depths were at 20.4 W/mm^2 and 35.6 W/mm^2 power levels which means that the peak point was around 25.5 W/mm^2 and 30.5 W/mm^2.

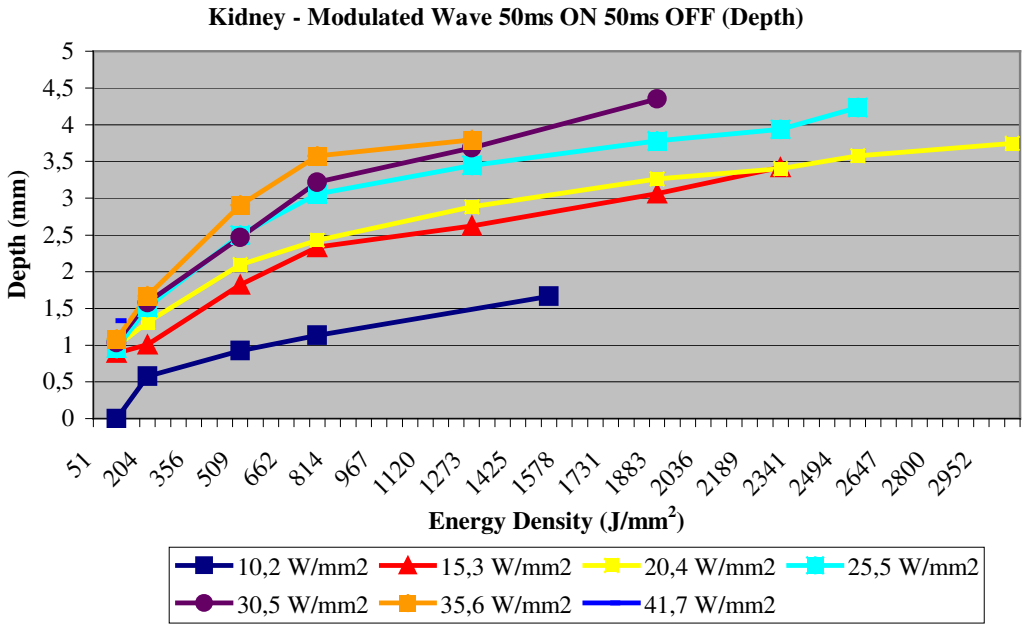

Figure 4.20 Applied power density, energy density and the corresponding lesion diameters

The best proposed dose for coagulation of kidney with 250 ms on/off modulated wave was 25.5 W/mm^2 2545 J/mm^2 The diameter of the coagulated zone was 6.25 mm with a standard deviation of 0.02 mm and the depth was 4.23 mm with a standard deviation of 0.07 mm.

4.3.4 Histology

Normal Kidney Histology	10.2 W/mm^2 2036 J/mm^2 (Continuous)
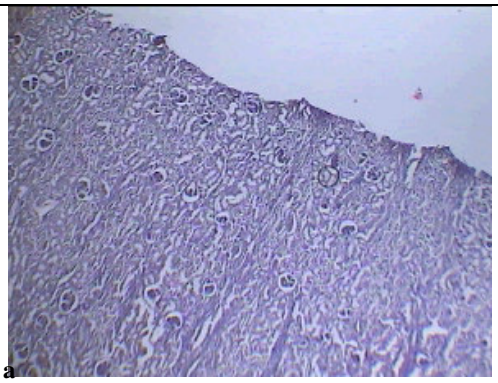 a	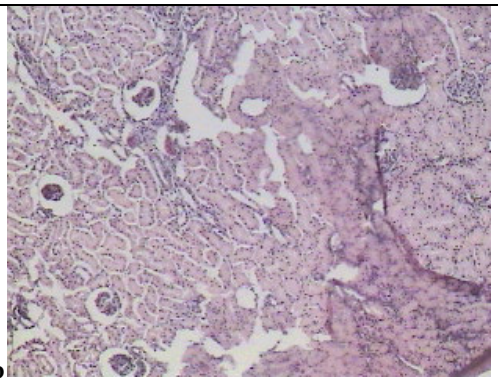 b
25.5 W/mm^2 2291 J/mm^2 (250ms ON/OFF)	**25.5 W/mm^2 2545 J/mm^2 (50ms ON/OFF)**
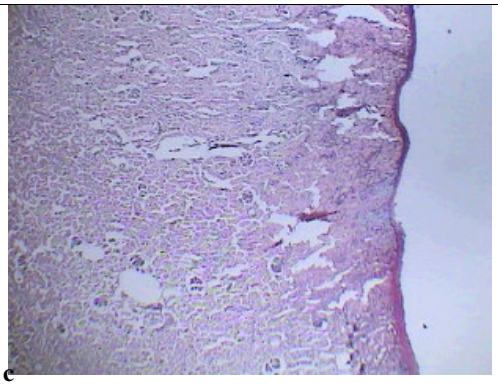 c	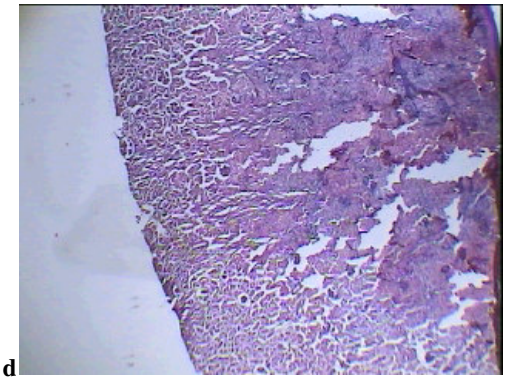 d

Figure 4.21 Histological sections for the chosen parameters for kidney. **a.** Normal kidney histology. **b.** Histology of kidney irradiated with continuous wave. **c.** Histology of kidney irradiated with 250ms on/off modulated wave. **d.** Histology of kidney irradiated with 50ms on/off modulated wave.

Thermal alteration of kidney was observed by histological analyses. The junctions between the cells were lost and tissue shrank. At the end of laser irradiations, largest coagulated zones were achieved in kidney experiments. After histological analyses, the clearest alterations were also observed on kidney.

4.4 Tissue Comparison

For soft tissue laser surgery, tissue type is one of the most effective parameters. Water, hemoglobin and melanin content of the tissue determine the thermal effects of the laser. Thus a specific laser has different effects on different tissues.

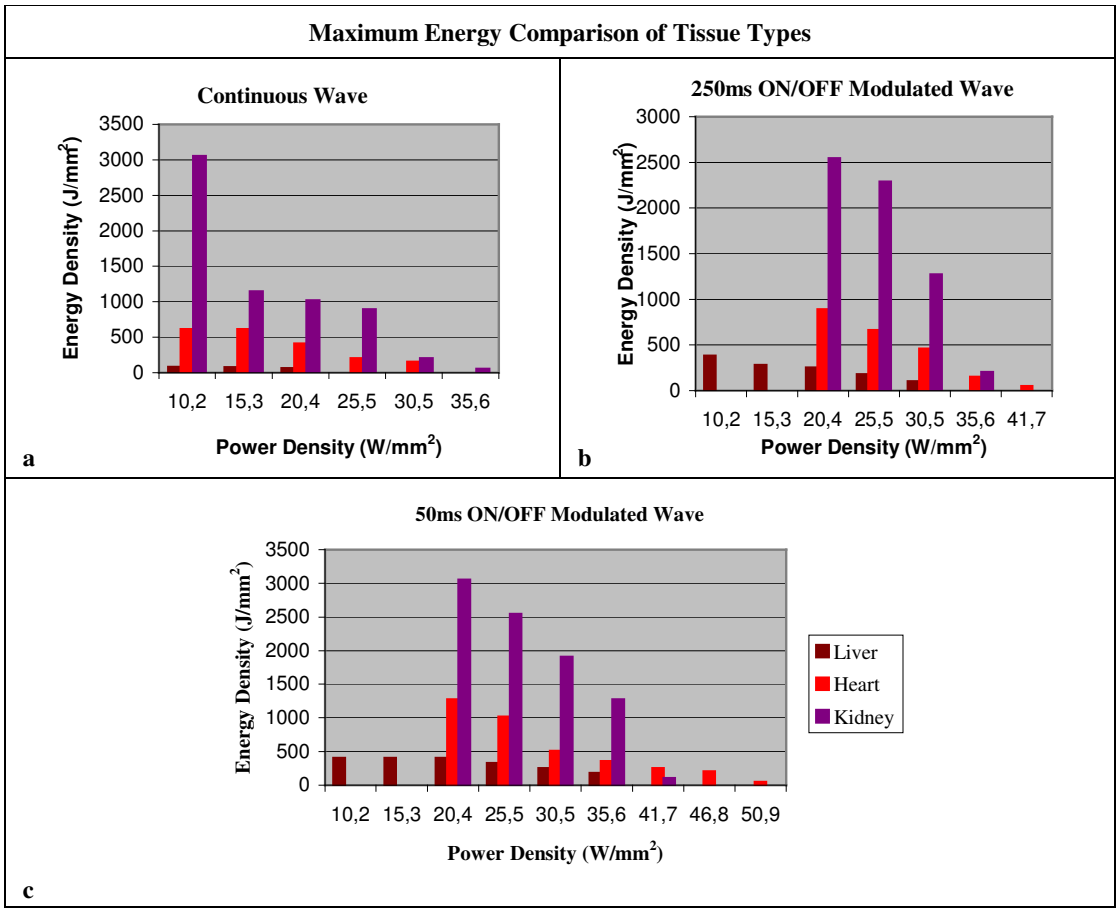

Figure 4.22 Maximum energy densities without carbonization at each power density and for each tissue type. **a.** Continuous Wave **b.** 250ms ON/OFF Modulated Wave **c.** 50ms ON/OFF Modulated Wave

Maximum energy densities at each power density were given for tissue types in Figure 4.22. In Figure 4.22 b-c the results of 10.2 W/mm^2 and 15.3 W/mm^2 were not given for heart and kidney because of the 5 minutes time limit. If modulation type was changed (Figure 4.22 a-b) maximum irradiance increased for all types of tissue. Maximum energy density also increased by changing the modulation type. Increasing the power density

decreased the carbonization threshold and maximum energy density for both modulation types and for both duty cycles (modulated wave).

Within modulated wave if on period was decreased (from 250 ms to 50 ms) maximum irradiance increased (Figure 4.22 b-c). Maximum energy density at a specific irradiance also increased by shorter duty cycles.

In between three tissues, kidney had the maximum energy density at low power (2 – 6 W, 10.2 – 30.5 W/mm^2). At high power (7 – 10 W, 35.6 – 50.9 W/mm^2) maximum energy density of kidney decreased rapidly compared to heart. Maximum power density for kidney was 41.7 W/mm^2 whereas it was 50.9 W/mm^2 for heart.

The water content of tissues were calculated by desiccation method, *in vitro* [18,22,23]. Eight samples from each tissue were taken, the tissues were then cut into small pieces to increase the surface area for evaporation and dried for 24 hours at 80 ^{o}C to constant weight. The difference between the wet weight and dry weight recorded as the water content of the tissue.

Water content of kidney and heart were almost equal (Table 4.2). Liver contained 20% less water when compared to heart and kidney. High water content of kidney and heart increased the absorption of the light energy. High specific heat capacity of water was the main reason of high energy density in heart and kidney compared to liver (Melanin c = 3.44 J/gK [24], Hemoglobin c= 2.88 J/gK [25], Water c = 4.19 J/gK [24]).

Water contents of lamb tissue and human tissue are on Table 4.2. The percentages were similar for heart and kidney. Taking into account the relatively high water absorption, 980 nm diode laser may have a future for human heart and kidney surgery.

Table 4.2
Water content of liver, heart, kidney for human [18] and lamb.

	Lamb			Human		
Water Content	**Liver**	**Heart**	**Kidney**	**Liver**	**Heart**	**Kidney**
Percentage (%)	66.5	78.6	79.3	75.1	75.8	78.3
St. Deviation (%)	1.1	0.9	0.7	2.1	4.5	0.7

In between three tissue types largest coagulated zones were achieved at kidney experiments, the second largest coagulations were at heart experiments. The smallest coagulated zones were at liver experiments. The results were summarized on Table 4.3.

Table 4.3
Maximum power density, maximum energy density, maximum diameter, maximum depth and proposed best doses for each type of tissue.

Mode	**Max. Power Density (W/mm^2)**	**Max. Energy Density (J/mm^2)**	**Max. Diameter (mm)**	**Max. Depth (mm)**	**Best Dose Proposed**			
					Power Density (W/mm^2)	**Energy Density (J/mm^2)**	**Diameter (mm)**	**Depth (mm)**
LIVER								
CW	20.4	81	2.65	1.19	15.3	76	2.65	1.19
250ms ON/OFF	30.5	382	3.80	2.03	10.2	382	3.80	1.86
50ms ON/OFF	46.8	407	4.00	2.54	15.3	407	4.00	2.54
HEART								
CW	30.5	611	4.47	2.54	15.3	611	4.47	2.54
250ms ON/OFF	41.7	1909	4.86	2.68	25.5	636	4.86	2.68
50ms ON/OFF	50.9	2291	5.22	3.22	25.5	1018	5.19	3,22
KIDNEY								
CW	35.6	3054	6.80	4.38	10.2	3054	6.80	4.38
250ms ON/OFF	35.6	2545	6.2	3.66	25.5	2291	6.2	3.66
50ms ON/OFF	41.7	3054	6.25	4.36	25.5	2545	6.25	4.23

5. DISCUSSION

Lasers have many advantages for surgery such as less operation time, faster healing and non-invasive or minimally invasive operations [11]. 980 nm diode laser has a larger water absorption coefficient ($H_2O\mu_a$) compared to other lasers working in the 800 – 1064 nm spectrum, its laser beam is transmissible through fiber, it makes minimal thermal damage to surrounding tissue and leads faster healing compared to electrosurgery in brain surgery [1]. Tissue temperature elevations are much greater when photons are well absorbed and confined to a small volume than when photons are poorly absorbed [6]. Thus 980 nm diode laser is a good alternative for soft tissue surgery.

The aim of this study was to investigate the *in vitro* effects of 980-nm diode laser on soft tissue (liver, heart, kidney). In this research study the main idea was to coagulate maximum area without carbonization in a limited time (maximum 5 minutes). Carbonization, which prolongs the healing of tissue, should be avoided in laser surgery [1]. 980-nm diode laser effects were investigated at non-contact mode at two different modalities; continuous wave and modulated wave (square, pulsed) with different parameters (output power of the laser, total energy delivered to the tissue, durations of on-off periods, and the number of on-off cycles for modulated wave). The effects of the light delivered to the tissue were investigated macroscopically; the diameter of coagulated tissue at the surface of the sample tissue and the depth of coagulation inside the sample tissue were measured by a digital calliper. Best proposed doses were chosen among the experimented doses and tissue samples were irradiated under proposed doses. 5 μm sections were taken by a microtome and thermal alteration was observed histologically.

The results of this study showed that the most important parameter for soft tissue coagulation is the type of modulation. For all kinds of tissue experimented, changing the modulation type increased the energy threshold for carbonization. Increasing the energy level causes wider and deeper coagulated zones. For example; liver has a carbonization threshold at 76 J/mm^2 for 15.3 W/mm^2 under continuous irradiation. It is 280 J/mm^2 for

250 ms on/off pulsed mode and 407 J/mm^2 for 50 ms on/off pulsed mode. The maximum diameter and maximum depth for continuous irradiation (15.3 W/mm^2) were 2.65 mm and 1,19 mm, respectively. The diameter and depth were increased to 3.31 mm and 1.92 mm for 250 ms on/off pulsed mode, respectively and 4.00 mm and 2.54 mm for 50 ms on/off pulsed mode, respectively. Since the carbonization thresholds increase, the risk for causing carbonization decreases by modulating the wave. The main reason of carbonization is the heat accumulated in the tissue. When the quantity of the heat energy given to the tissue is larger than the conduction of the heat energy to nearby tissue, the excessive amount accumulates in the tissue. This condition leads to rapid increases of the temperature of that region. This temperature increase causes carbonization.

Above 30.5 W/mm^2, the curves are almost linear (Figures 4.5, 4.6, 4.12, 4.13, 4.20, 4.21). It is because of the high power density of the irradiation. Below 35.6 W/mm^2, tissue shrinks indicating the water evaporation but at high power tissue does not shrink, focal point size and the power density stays constant. The temperature increase is so rapid that tissue is coagulated before the evaporation of water. For continuous irradiation because of high energy density, maximum power does not exceed 35.6 W/mm^2. On the other hand, for modulated wave, off periods let the conduction of the heat energy. The energy spread over the tissue and the temperature increase slows down, letting to increase the maximum power without carbonization.

Changing the duration of the duty cycle also affects the carbonization threshold. Setting the duty cycle low (50 ms) instead of high (250 ms) increases the carbonization threshold. For example, at 20.4 W/mm^2 the carbonization threshold increased from 255 J/mm^2 to 407 J/mm^2 for liver, from 891 J/mm^2 to 1272 J/mm^2 for heart and from 2545 J/mm^2 to 3054 J/mm^2 for kidney. For all types of tissue the threshold energy for carbonization, the diameters and the depths increased when the duty cycle was changed to 50 ms from 250 ms. It is obvious that there are more reliable results when the duty cycle duration is set to 50 ms instead of 250 ms. For future work many sets of on/off periods should be experimented. The comparison of different modulated wave types may contribute to the coagulation process of the soft tissue.

Another parameter that affects the area of the coagulated zone is output power. The advantages of higher power levels are shorter operation time and larger coagulation area. The reason for larger coagulation zone is fast heat transfer within the tissue and rapid temperature elevation of the tissue [6]. The disadvantage of high power is the risk of carbonization of the target and thermal alteration of the adjacent tissue; therefore working at low powers (10.2 – 30.5 W/mm^2) is safer than high power (35.6 – 50.9 W/mm^2). The position of the fiber during laser surgery is critical; it can be used interstitially, in touch or non-touch mode.

Focal spot size, which was 500μm, is an important parameter for irradiance. Irradiance, also called power density, is a measurement of the rate of work within a defined area and is generally reported as W/cm^2 [6]. To simplify the results, W/mm^2 for irradiance and J/mm^2 for energy density were used in this research study.

Heat conduction is the primary mechanism by which heat is transferred to unexposed tissue structures [5]. On the surface of the sample tissue, the beam diameter was 0,5 mm, whereas the diameter of the coagulated zone increased up to 6 mm. The first mechanism that increases the coagulation diameter on the surface from 0.5 mm to 6 mm is the heat conduction. Heat generated on the surface by absorbing light energy is conducted to nearby tissue. The second mechanism is the scattering of the beam. When laser beam hits the surface of the target tissue, some of the photons are scattered over the surface. Some of these scattered photons are absorbed by nearby tissue and heat is generated, increasing the temperature of nearby tissue.

In most biological tissues, it was found by Wilson and Adam (1983) that photons are preferably scattered in the forward direction. For anisotropic scattering (g scattering), the coefficient of anisotropy g is defined, where $g = 1$ denotes purely forward scattering, $g = -1$ denotes purely backward scattering. It can be assumed that g ranges from 0.7 to 0.99 for most biological tissues [5]. 980 nm diode laser has a penetration depth around 2 mm for soft tissue [21], but the depth of the coagulated zone was 4 mm maximum. Thus, g scattering is an important mechanism for coagulation of deeper tissue.

Tissue type by itself is one of the most effective parameters for soft tissue surgery during laser surgery. Tissue properties (hemoglobin, melanin and water content) determine the response of the tissue to the laser. Since water has a local absorption peak at 980 nm, water content of the tissue determines the heat effect on the tissue for 980-nm diode laser.

In between three different tissues (liver, heart and kidney) the amount of energy needed to coagulate same amount of tissue is least for liver. To coagulate same amount of tissue 40% of the energy needed by heart or kidney is enough for liver. The results are supported by the water content of the tissues (Table 4.2). Liver contains the least water 66.5% and has the least maximum energy density. Heart and kidney show similar characteristics and their water content are almost equal (heart 78.6%, kidney 79.3%).

The thermal alteration of tissues are observed after histological analyses. Liver tissue shrank and cells formed groups with spacing between them (Figure 4.7). The junction between endocardium and myocardium cannot be observed for heart after histological analyses (Figure 4.14). For kidney, the junction between the cells were lost and the tissue shrank (Figure 4.21).

The intrinsic variability of human tissue makes it difficult to define strict treatment protocols. Individual variations in blood supply influence the eventual clinical effect. A high local blood flow is likely to lead to dissipation of heat away from the tissue and reduce the effectiveness of the treatment [12]. The water content of human tissue was reported as, liver 75%, heart 76% and kidney 78%, average [18]. Taking into account the water absorbance at 980 nm and the water content of human tissue, 980 nm diode laser may be o good alternative for soft tissue surgery on humans. On the other hand, thermal tissue coagulation leads to considerable changes in the optical parameters during irradiation. After coagulation, the absorption coefficient and anisotropy factor decrease, while the scattering coefficient increases [21]. Thus, there is the demand that the application parameters should not be kept constant for the entire application. They should be continuously or gradually adapted during therapy in order to achieve the maximum treatable lesion volume.

6- CONCLUSION

The parameters of 980-nm diode laser for soft tissue surgery were investigated. The results of two different modes (continuous wave and modulated wave; 250ms on/off, 50ms on/off) were reported and the carbonization thresholds for each power level were mentioned. Below carbonization threshold the diameters and the depths of the coagulated zone were measured and the average values with standard deviations were calculated. Best proposed doses were determined for maximum area of the coagulated zone. Finally the thermal changes of the tissue were shown by histological analyses.

The experiments successfully showed that each kind of tissue (liver, heart and kidney) could be coagulated by 980 nm diode laser. The largest coagulated zones were on kidney, then heart and finally on liver. The resulting diameters of the coagulated tissue increased up to 6 mm and the depths to 4 mm for kidney. Since the coagulated zones were circular the largest area calculated was 113 mm^2. Largest coagulations were in kidney experiments. Water content of human kidney is 78.3% and lamb kidney is 79.3%, thus 980 nm diode laser may have a future for treating the cists on human kidney.

These *in vitro* experiments are important for future investigations of 980-nm diode laser over soft tissue, especially for *in vivo* experiments. The results will be a guide for the research of heat conduction through soft tissue that has just started in our biophotonics laboratory.

APPENDIX A. LIVER

A.1 Continuous Wave

Table A.1
Liver continuous wave graphs. Diameter – Energy Density and Depth – Energy Density Graphs for each power density.

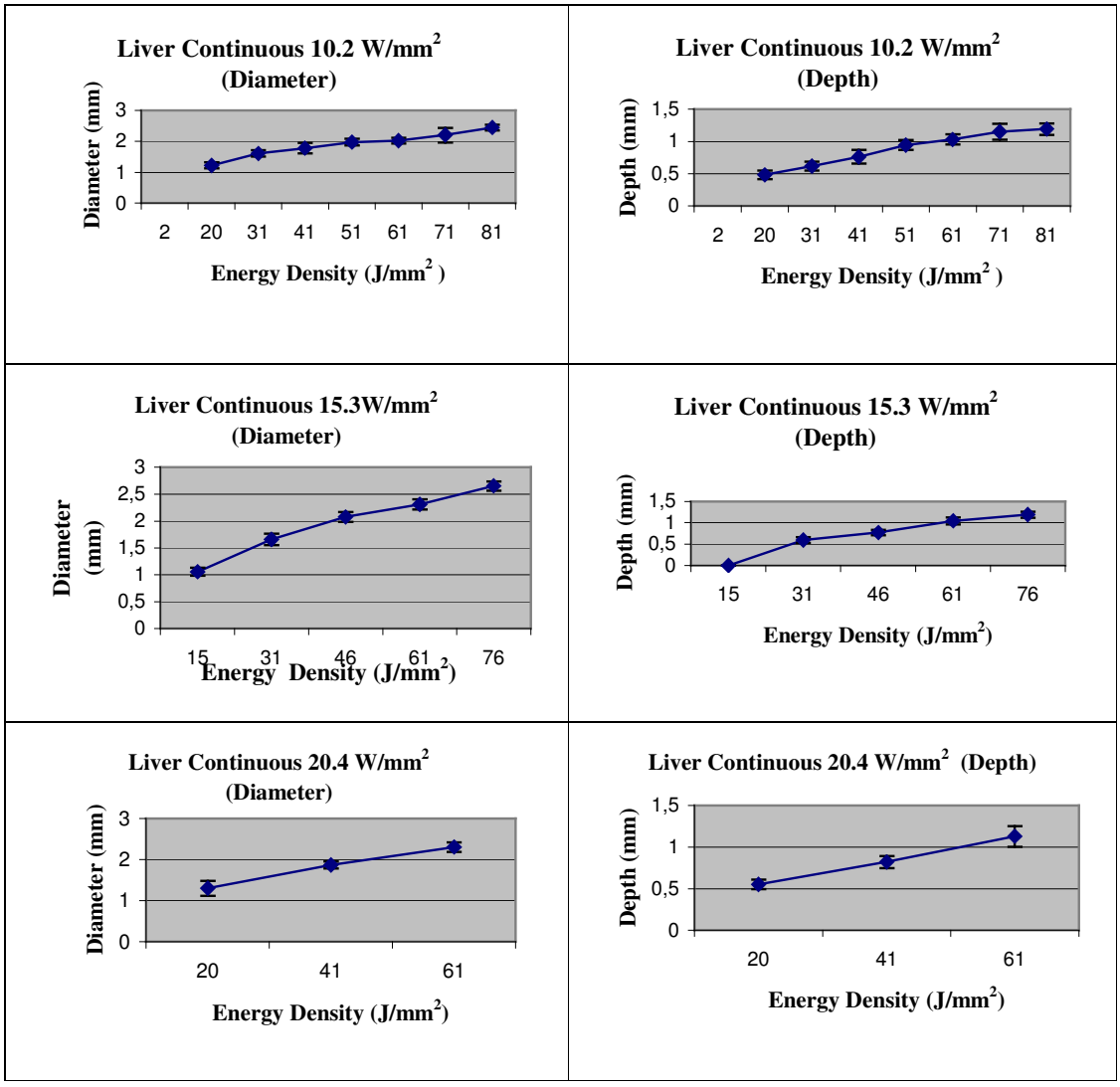

A.2 250 ms ON/OFF Modulated Wave

Table A.2
Liver 250 ms on/off modulated wave graphs. Diameter – Energy Density and Depth – Energy Density Graphs for each power density.

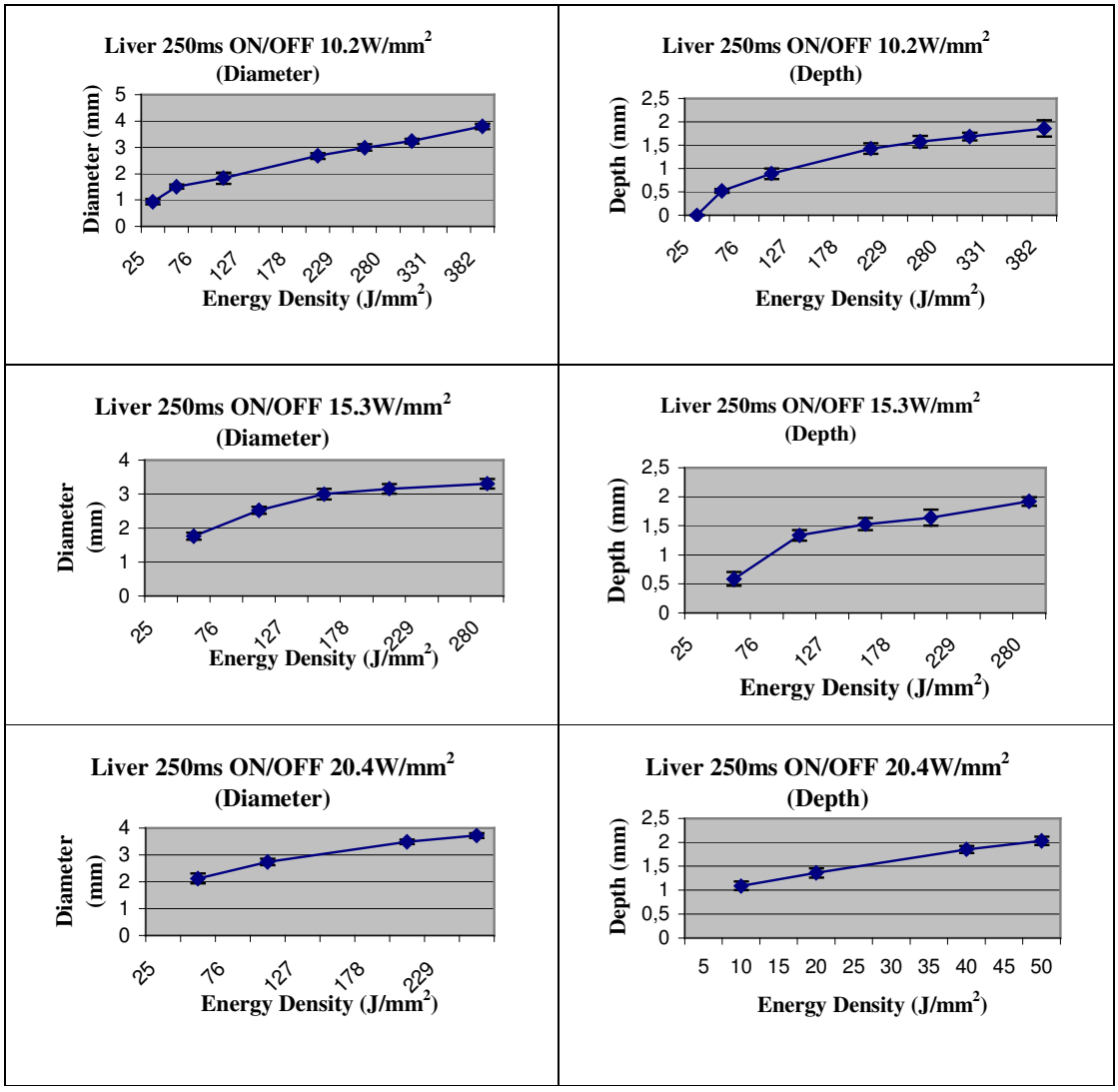

Table A.2 (Continued)
Liver 250 ms on/off modulated wave graphs. Diameter – Energy Density and Depth – Energy Density Graphs for each power density.

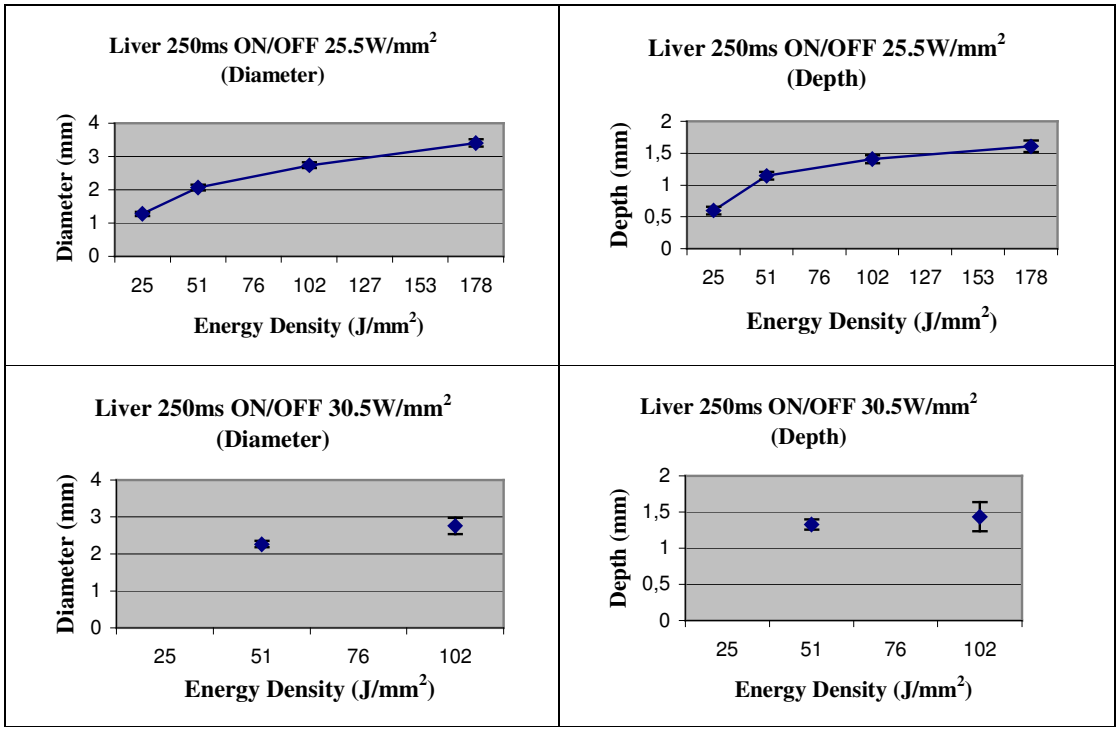

A.3 50 ms ON/OFF Modulated Wave

Table A.3
Liver 50 ms on/off modulated wave graphs. Diameter – Energy Density and Depth – Energy Density Graphs for each power density.

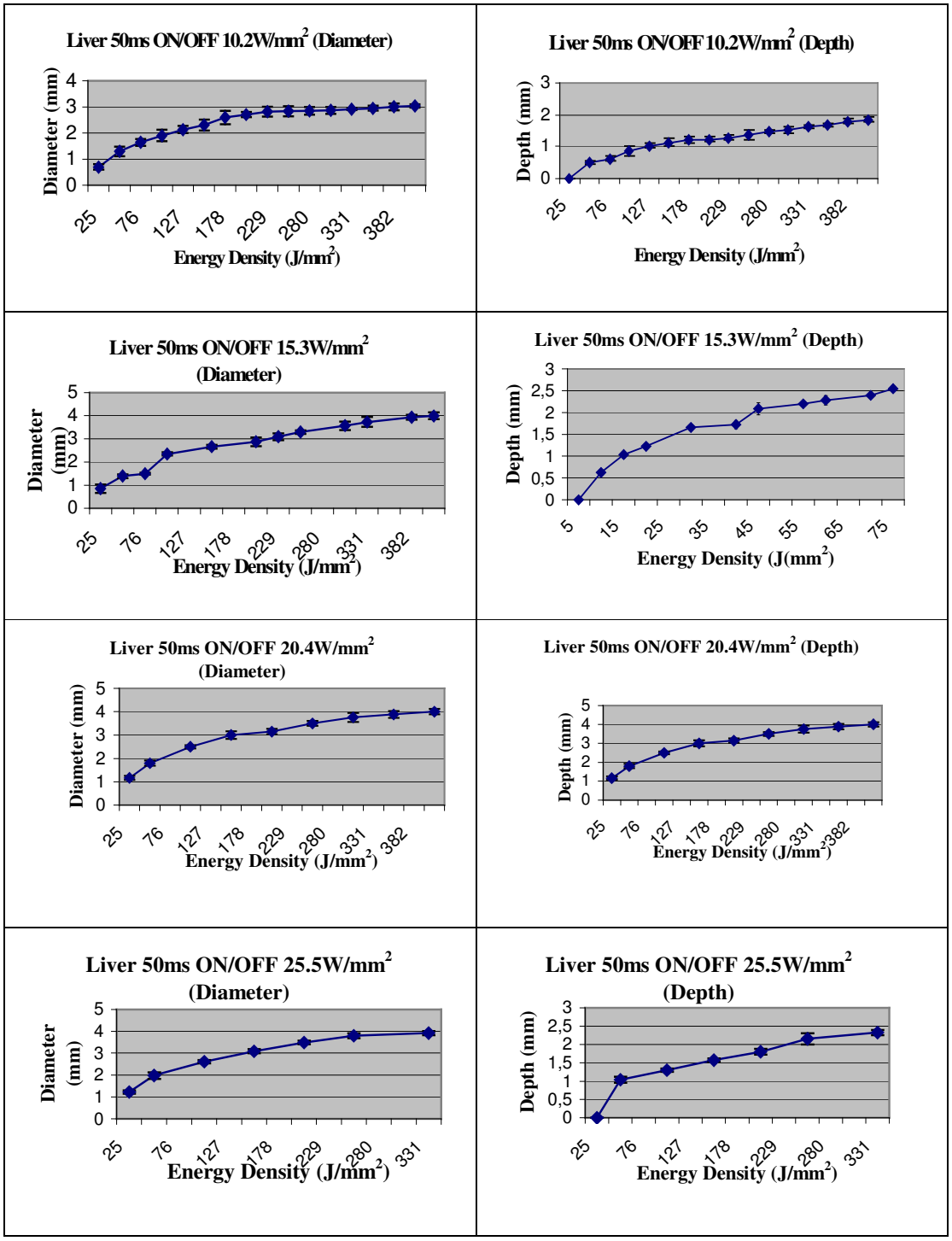

Table A.3 (Continued)

Liver 50 ms on/off modulated wave graphs. Diameter – Energy Density and Depth – Energy Density Graphs for each power density.

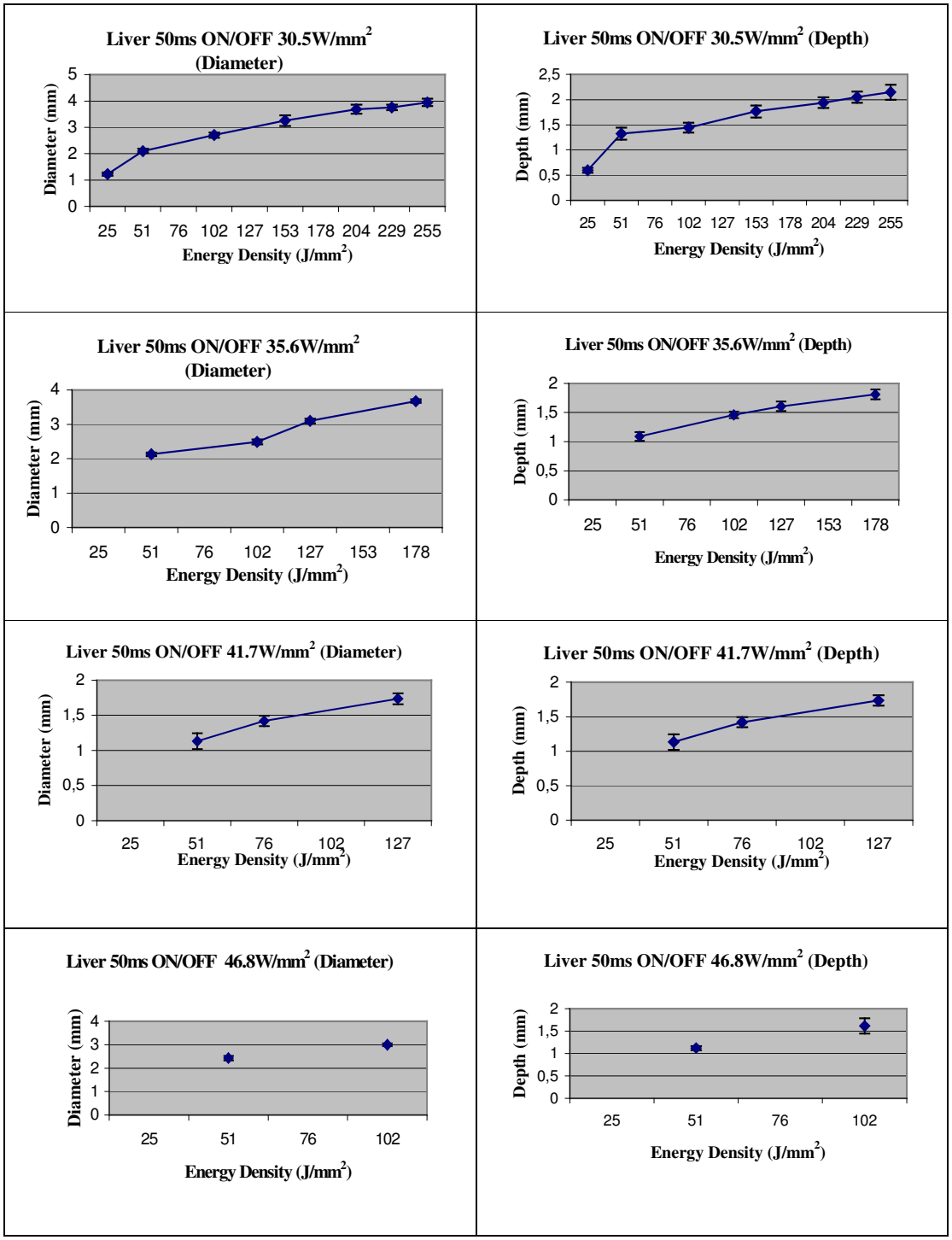

APPENDIX B. HEART

B.1 Continuous Wave

Table B.1
Heart continuous wave graphs. Diameter – Energy Density and Depth – Energy Density Graphs for each power density.

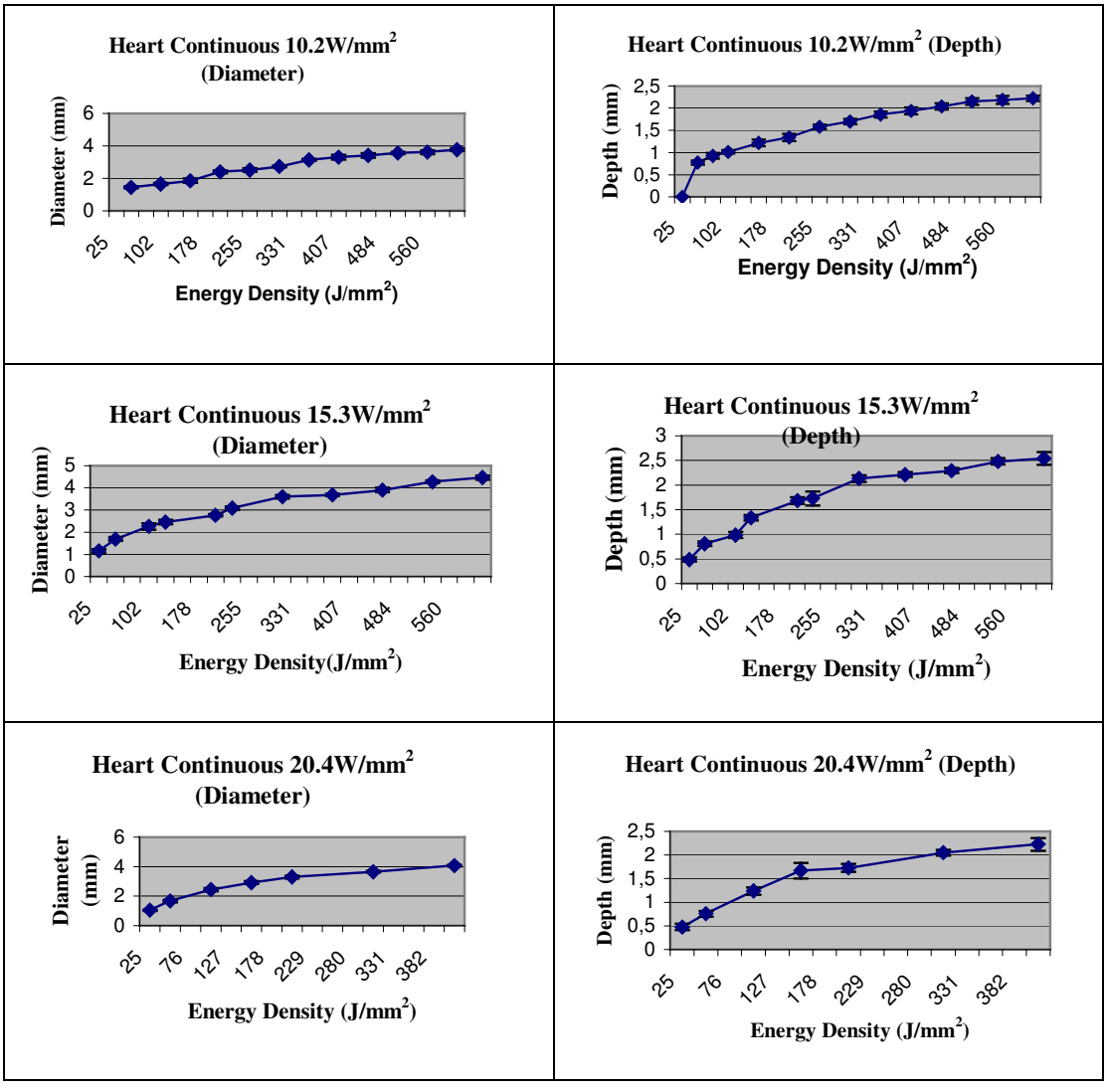

Table B.1 (Continued)
Heart continuous wave graphs. Diameter – Energy Density and Depth – Energy Density Graphs for each power density.

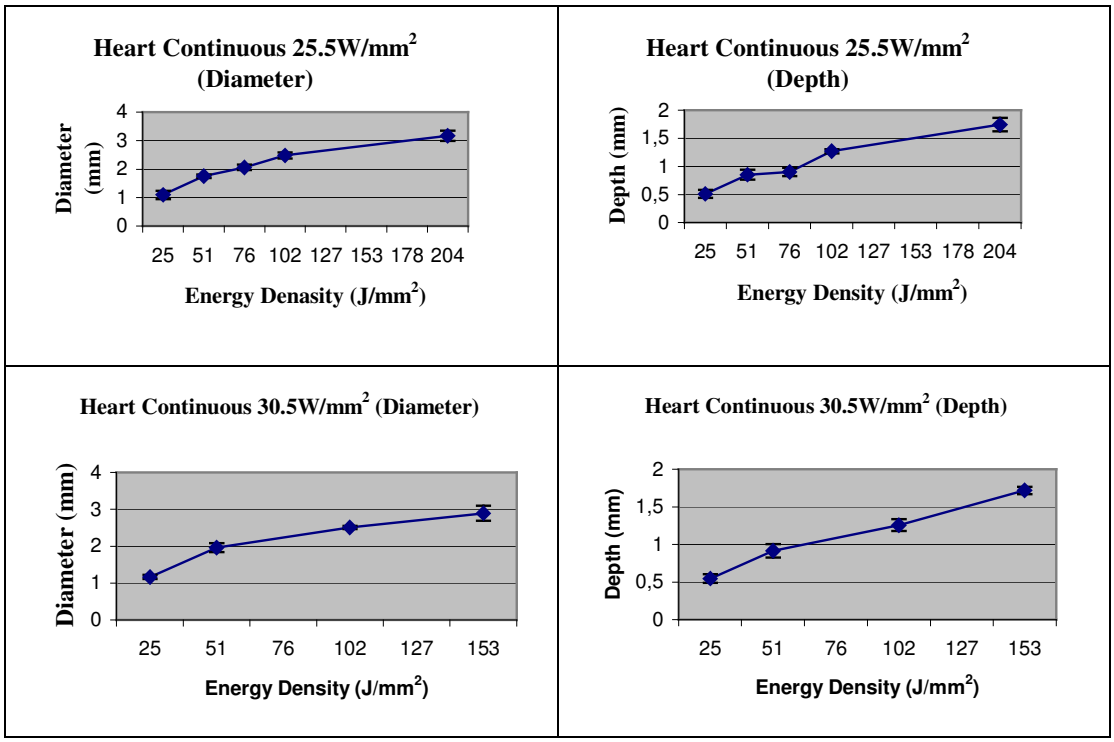

B.2 250 ms ON/OFF Modulated Wave

Table B.2
Heart 250 ms on/off modulated wave graphs. Diameter – Energy Density and Depth – Energy Density Graphs for each power density.

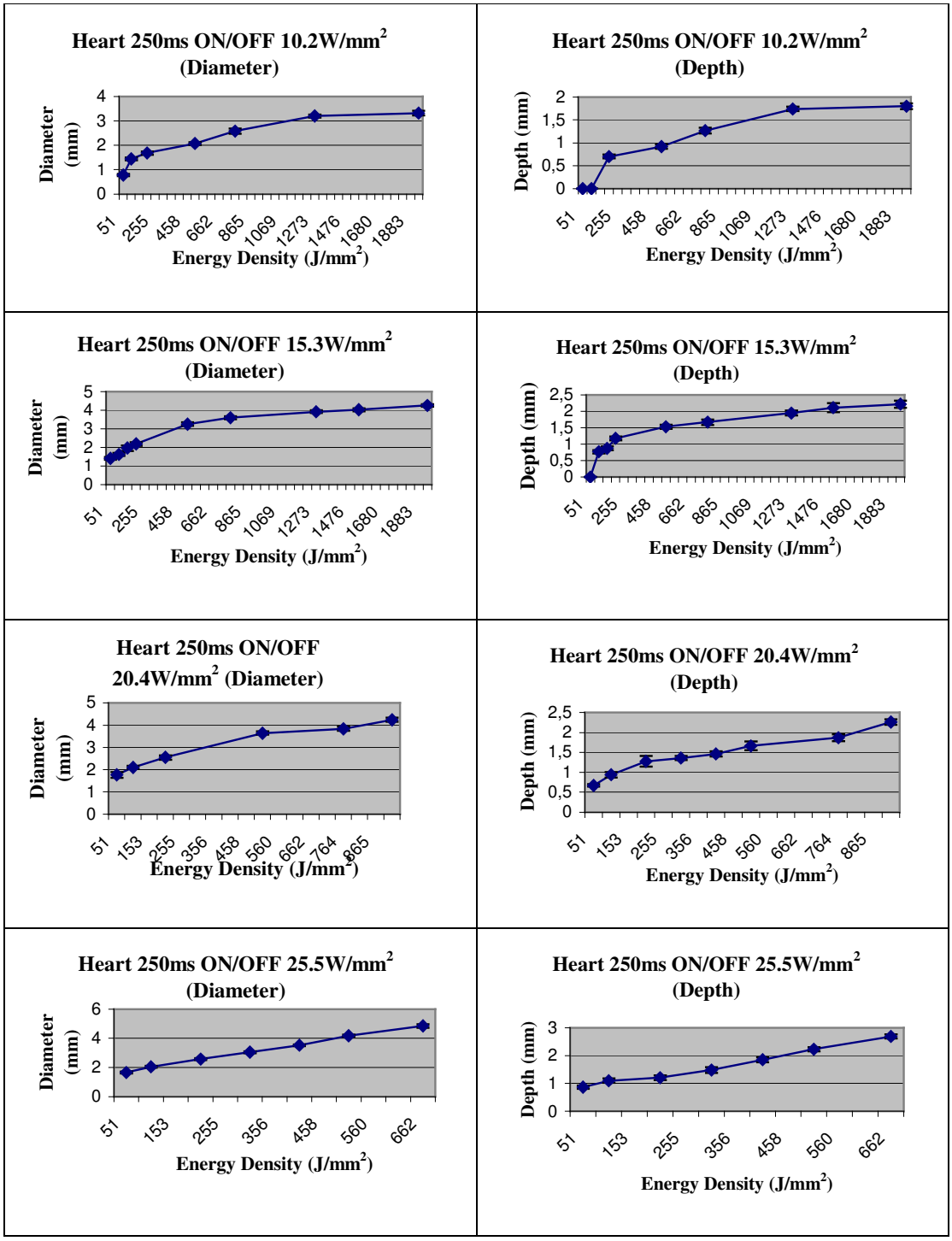

Table B.2 (Continued)
Heart 250 ms on/off modulated wave graphs. Diameter – Energy Density and Depth – Energy Density Graphs for each power density.

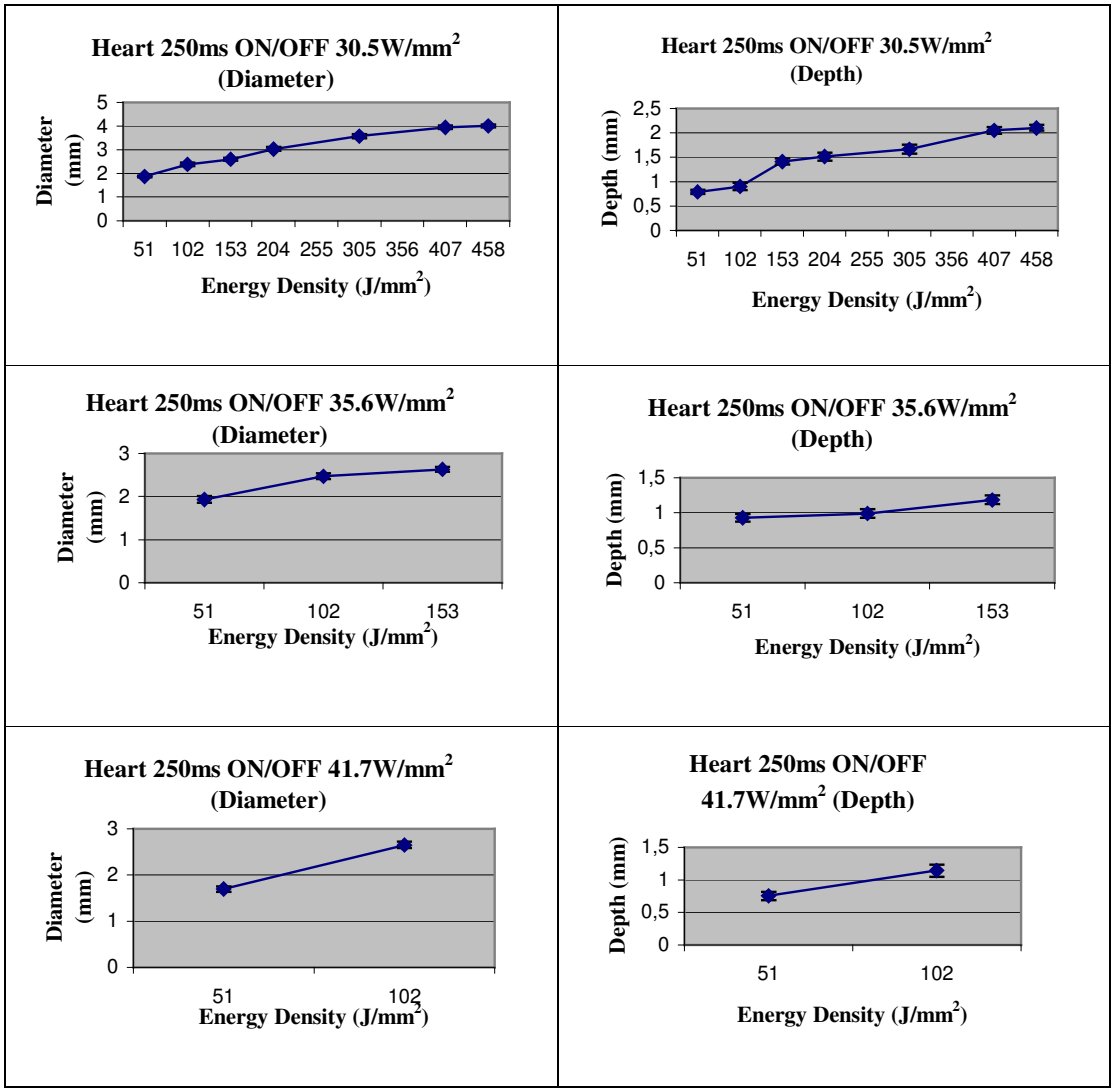

B.3 50 ms ON/OFF Modulated Wave

Table B.3
Heart 50 ms on/off modulated wave graphs. Diameter – Energy Density and Depth – Energy Density Graphs for each power density.

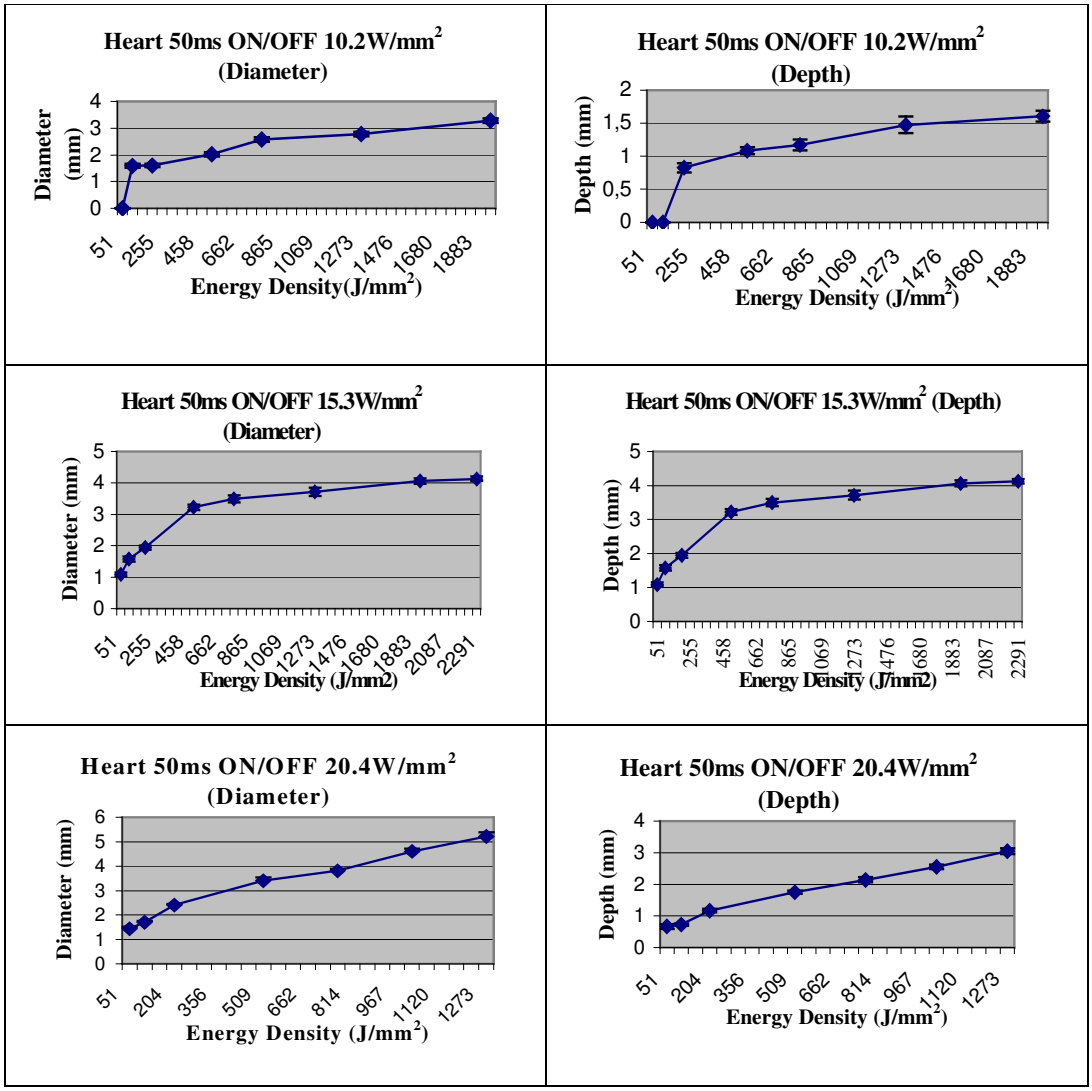

Table B.3 (Continued)

Heart 50 ms on/off modulated wave graphs. Diameter – Energy Density and Depth – Energy Density Graphs for each power density.

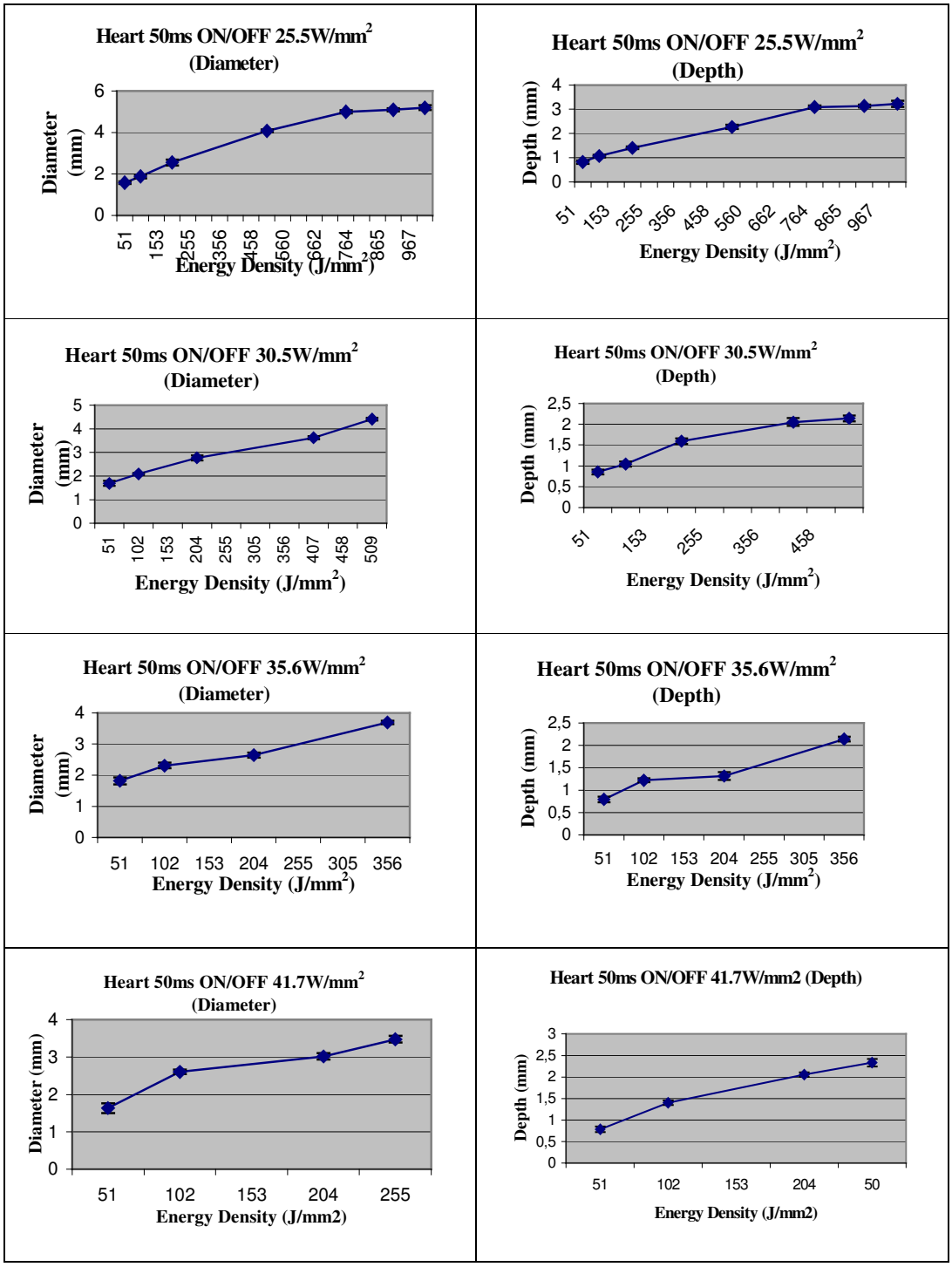

Table B.3 (Continued)

Heart 50 ms on/off modulated wave graphs. Diameter – Energy Density and Depth – Energy Density Graphs for each power density.

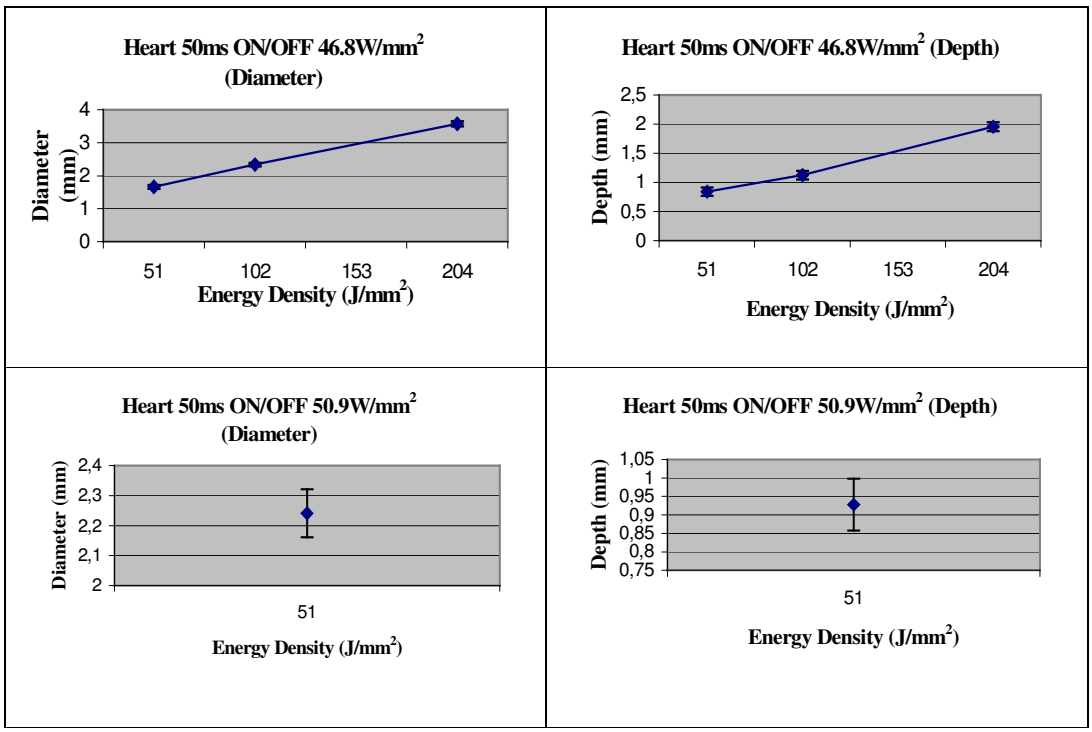

APPENDIX C. KIDNEY

C.1 Continuous Wave

Table C.1
Kidney continuous wave graphs. Diameter – Energy Density and Depth – Energy Density Graphs for each power density.

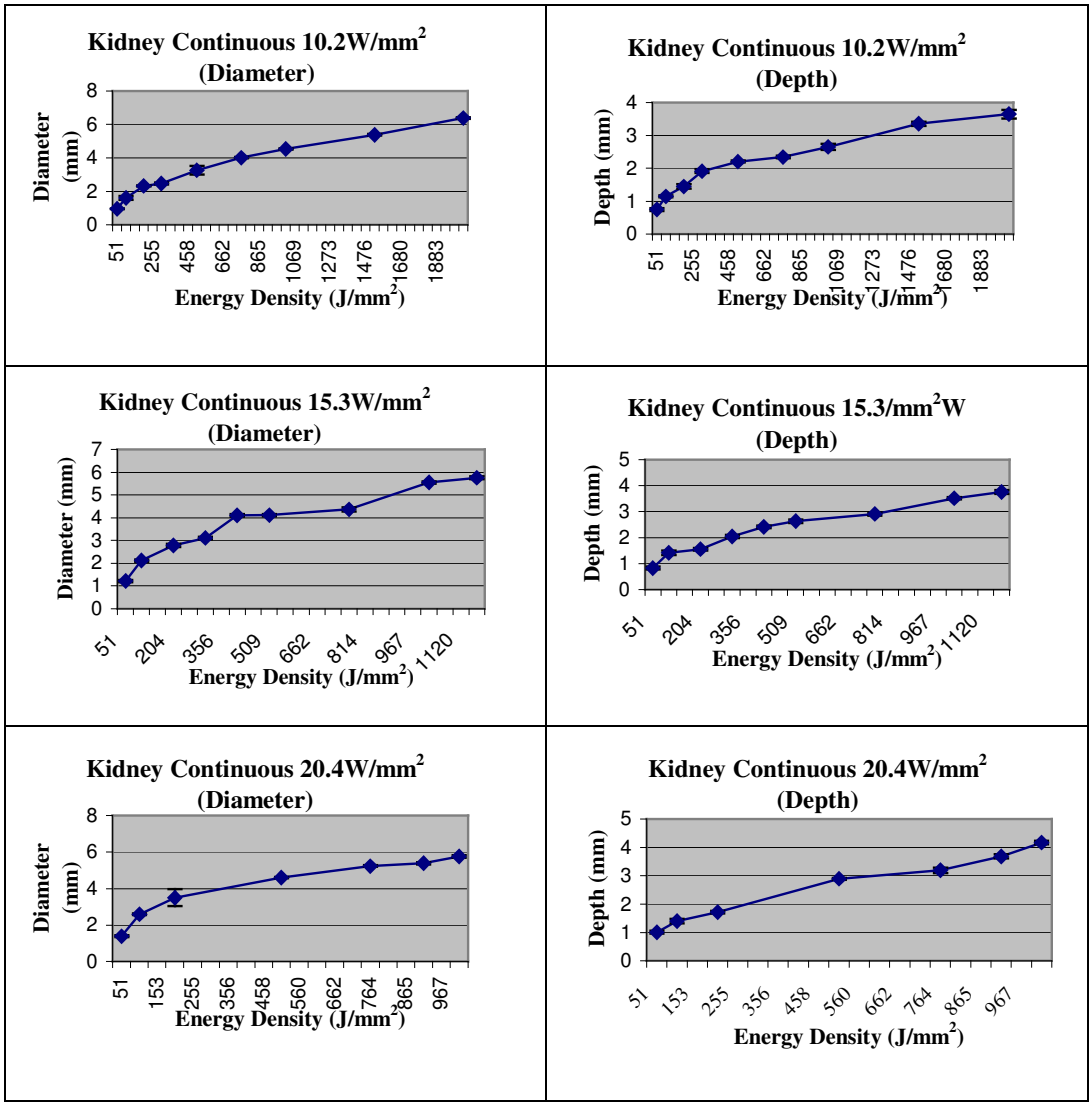

Table C.1 (Continued)
Kidney continuous wave graphs. Diameter – Energy Density and Depth – Energy Density Graphs for each power density.

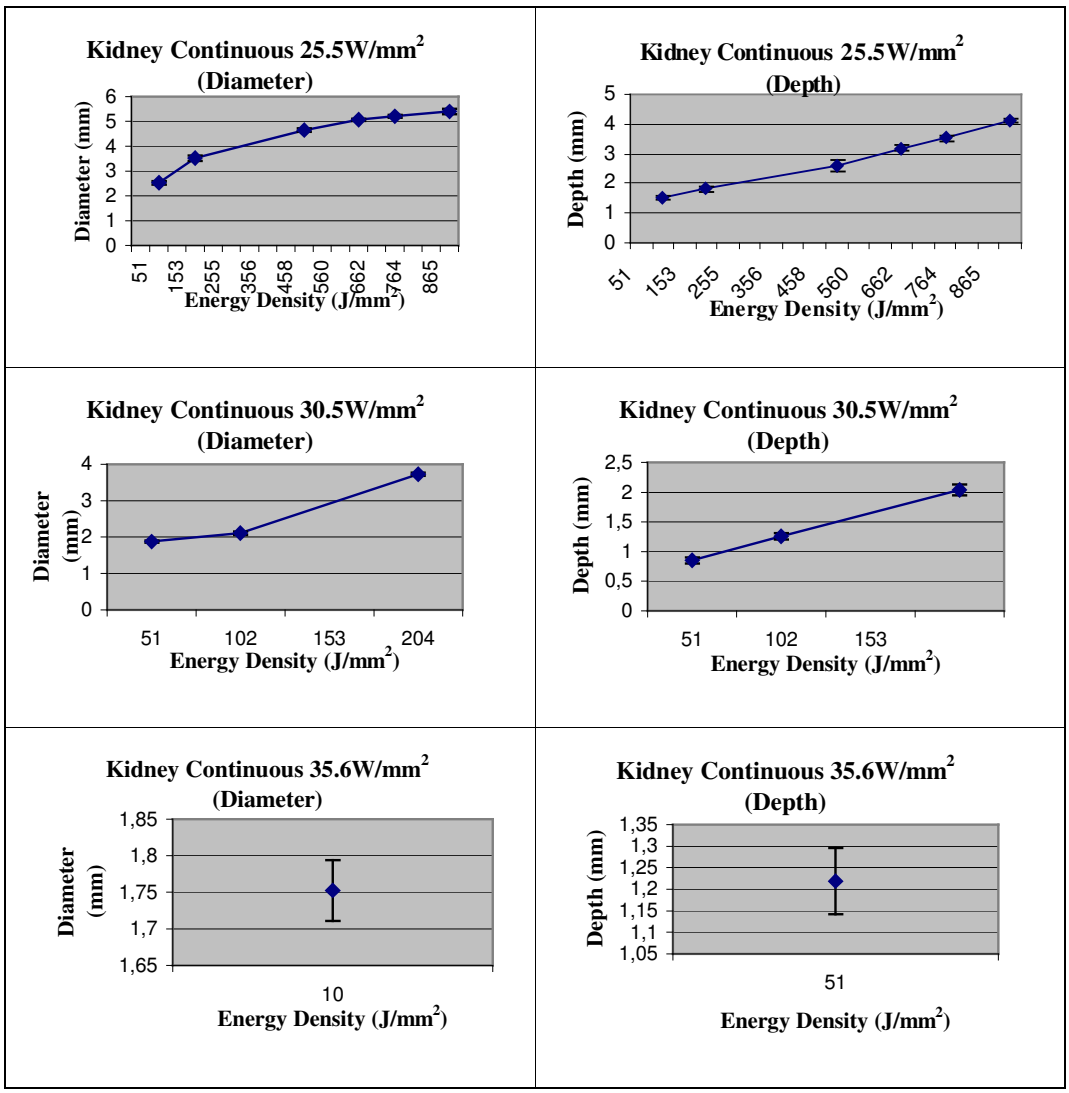

C.2 250 ms ON/OFF Modulated Wave

Table C.2
Kidney 250 ms on/off modulated wave graphs. Diameter – Energy Density and Depth – Energy Density Graphs for each power density.

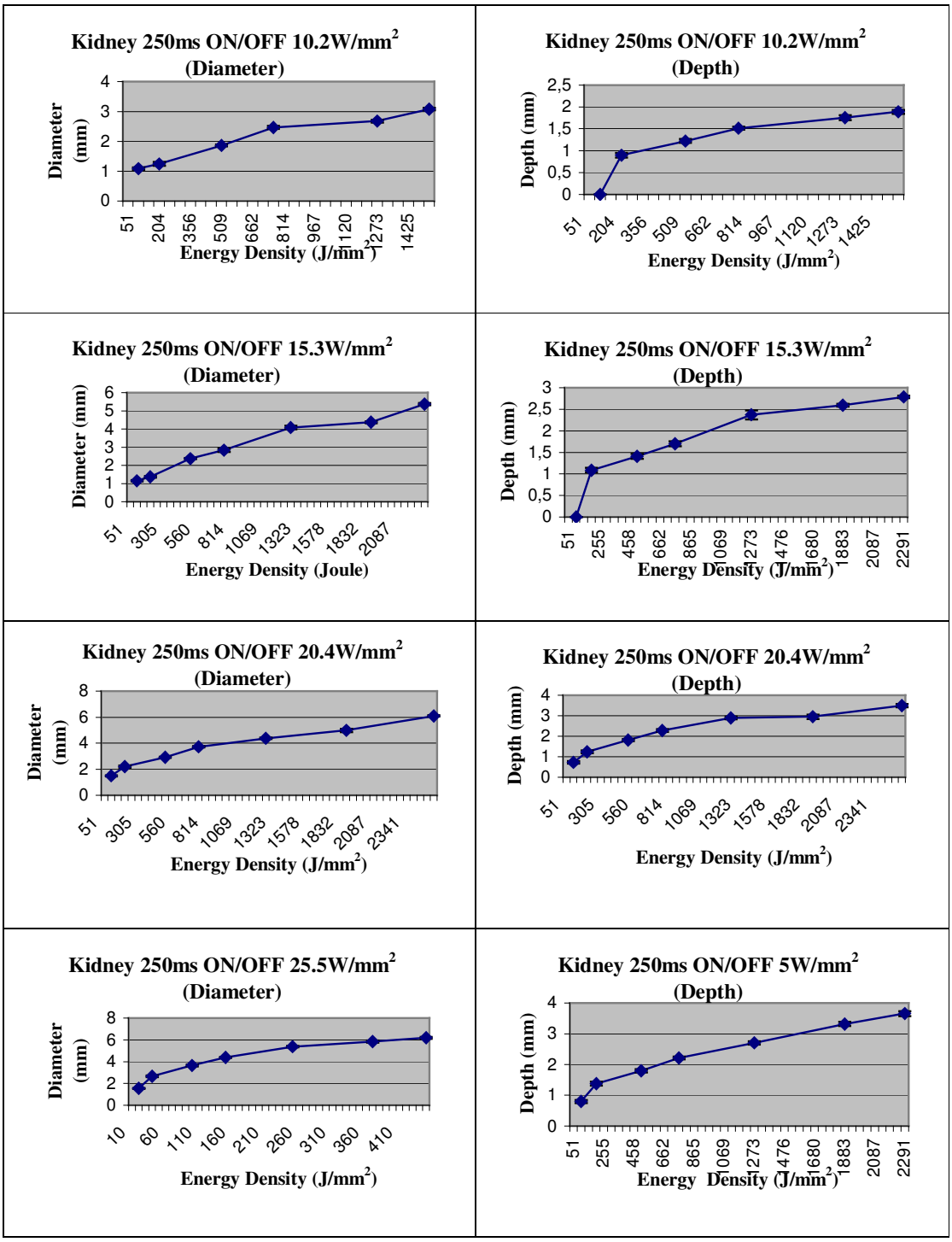

Table C.2 (Continued)
Kidney 250 ms on/off modulated wave graphs. Diameter – Energy Density and Depth – Energy Density Graphs for each power density.

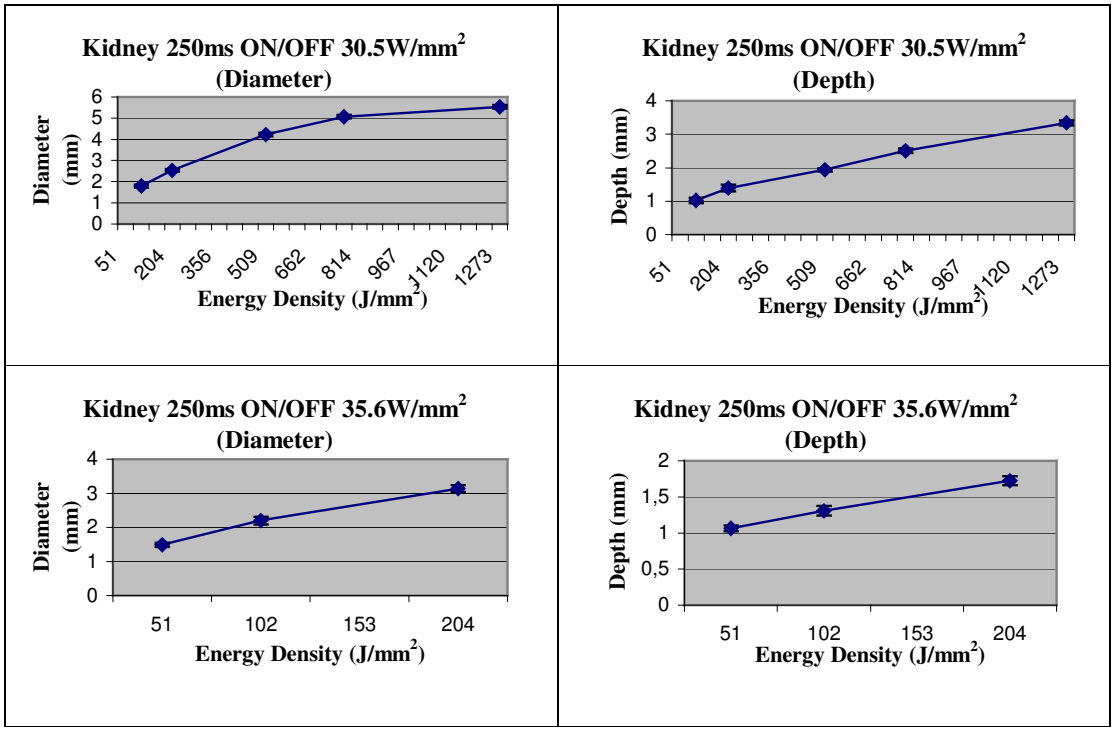

C.3 50 ms ON/OFF Modulated Wave

Table C.3
Kidney 50 ms on/off modulated wave graphs. Diameter – Energy Density and Depth – Energy Density Graphs for each power density.

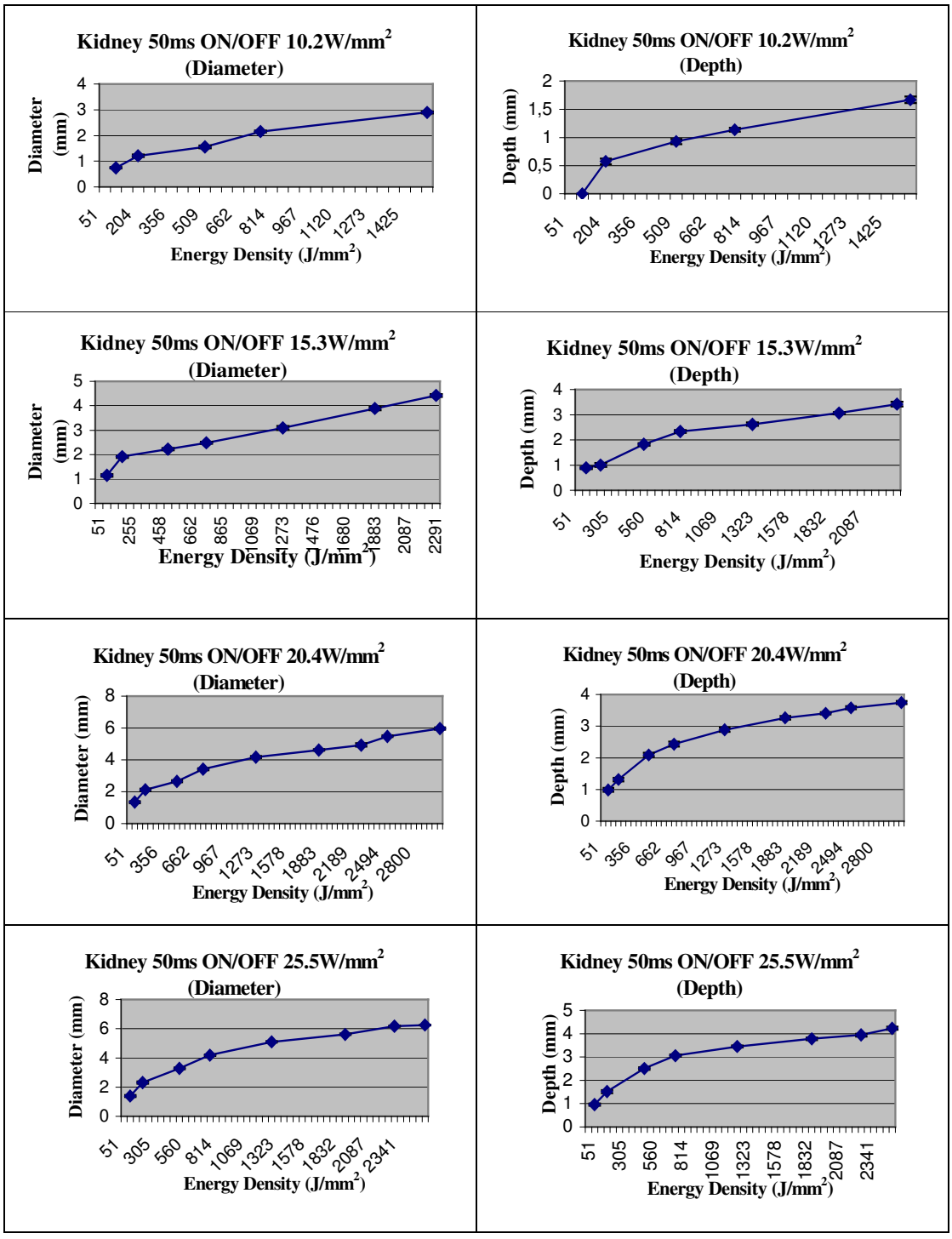

Table C.3 (Continued)
Kidney 50 ms on/off modulated wave graphs. Diameter – Energy Density and Depth – Energy Density Graphs for each power density.

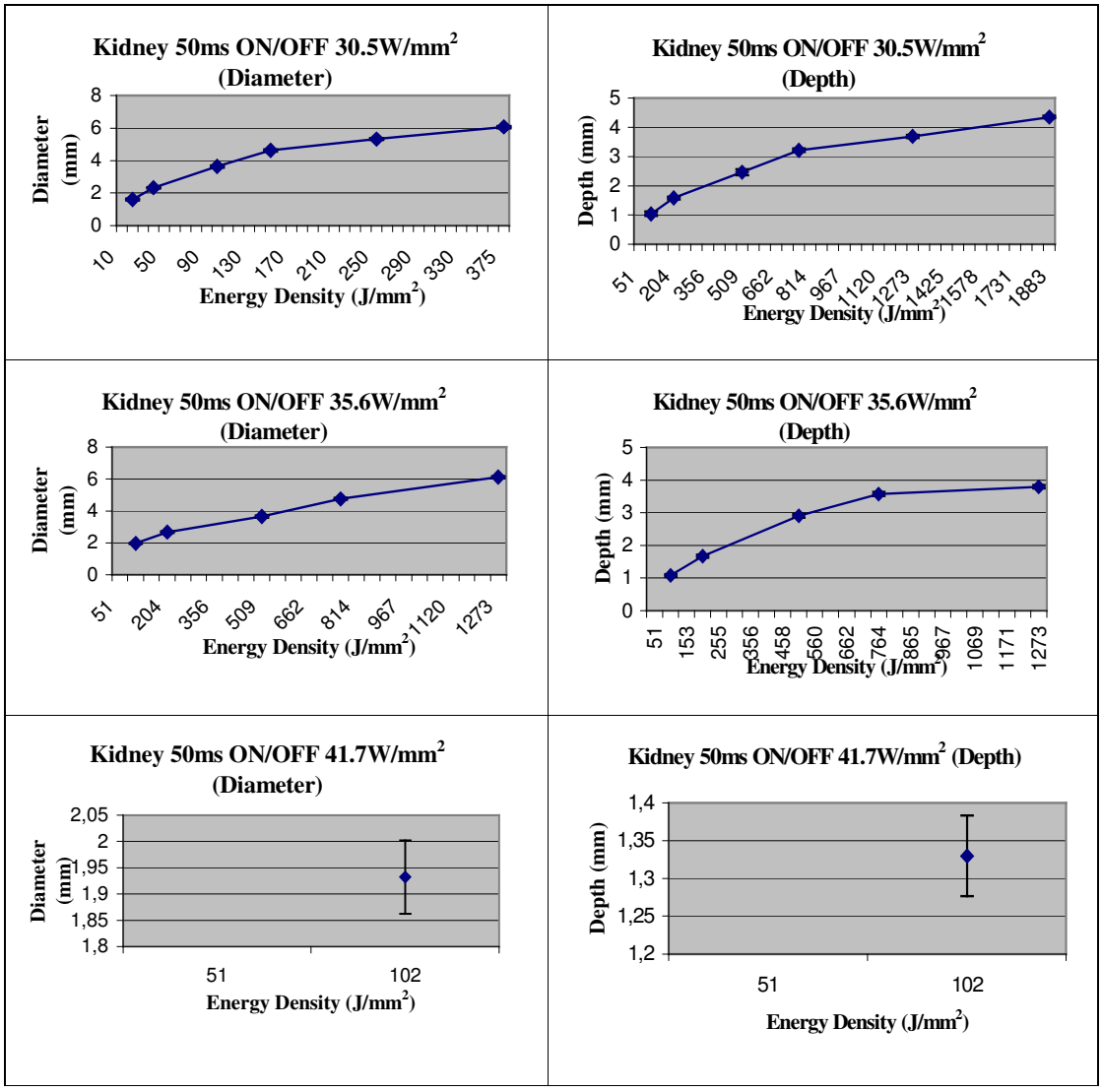

REFERENCES

1. Bozkulak, O., H. O. Tabakoglu, A. Aksoy, O. Kurtkaya, A. Sav, R. Canbeyli, M. Gulsoy, "The 980-nm diode laser for brain surgery: histopathology and recovery period," *Lasers in Medical Science*, Vol. 19, pp. 41-47, 2004.

2. Ware, D. L., P. Boor, C. Yang, A. Gowda, J. J. Grady, M. Motamedi, "Slow Intramural Heating With Diffused Laser Light," *Circulation*, Vol. 99, pp. 1630-1636, 1999.

3. Germer, C.T., D. Albrecht, C. Isbert, J. Ritz, A. Roggan and H.J. Buhr," Diffusing Fibre tip for the minimally invasive treatment of liver tumours by interstitial laser coagulation," *Lasers in Medical Science* Vol. 14, pp. 32-39, 1999.

4. Martin, J.C. and A.J.Welch, "Clinical Use Of Laser-Tissue Interactions," *IEEE Engineering in Medicine and Biology Magazine* Vol. 8, pp. 10-13, 1989.

5. Niemz, M.H., *Laser Tissue Interactions, Fundamentals and Applications*, Germany: Springer, Third Edition, 1996.

6. Peavy,G.M., "Lasers and laser-tissue interaction," *The Veterinary Clinics Small Animal Practice* Vol. 32, pp. 517-534, 2002.

7. Sullins, K.E., "Diode laser and endoscopic laser surgery," *The Veterinary Clinics Small Animal Practice* Vol. 32, pp. 639-648, 2002.

8. El-Sherif, A. F., T. A. King, "Soft and hard tissue ablation with short-pulse high peak power and continuous thulium-silica fibre lasers," *Lasers in Medical Science*, Vol. 18, pp. 139-147, 2003.

9. K.R. Goebel, "Fundamentals of Laser Science," *Actaneurochir. Suppl.* Vol. 61, pp. 20-33, 1994.

10. White J.M., S.I., Chaudhry, J.J. Kudler, N. Sekandari, M.L. Schoelch, S.Jr. Silverman, "Nd:YAG and CO2 laser therapy of oral mucosal lesions," *J Clin Laser Med Surg.*, Vol. 16, pp. 299-304, December 1998.

11. Gulsoy M., Z. Dereli, H.O. Tabakoglu, O. Bozkulak, "Closure of skin incisions by 980-nm diode laser welding," *Lasers in Medical Science*, Vol. 21, pp. 5-9, April 2006.

12. Anson K, G. Buonnaccorsi, M. Eddowes, S. MacRobert, T. Mills, G. Watson, "A comparative optical analysis of laser sidefiring devices: a guide to treatment," *Br J Urol*, Vol. 75, pp. 328-334, 1995.

13. Welch A.J., J,H. Torres, W.F. Cheong, "Laser Physics and Laser-Tissue Interaction," *Texas Heart Institute Journal*, Vol. 16, pp. 141-149, 1989.

14. Gulsoy, M., T.A. Celikel, O. Kurtkaya, A. Sav, A. Kurt, R. Canbeyli, I. Cilesiz, "Application of the 980-nm diode laser in stereotactic surgery," *IEEE Journal of Selected Topics in Quantum Electronics*, Vol. 5(2), pp. 1090-1094, 1999.

15. Bartels, K.E., "Lasers in Medicine and Surgery," *The Veterinary Clinics Small Animal Practice*, Vol. 32, pp. 517-534, 2002.

16. Svelto, O., *Principles of Lasers*, New York: Plenum Press, 1998.

17. Bozkulak O., H.O. Tabakoglu, A. Aksoy, N. Bilgin, R. Canbeyli, O. Kurtkaya, A. Sav, M. Gulsoy, "Investigating the recovery period of rat brain tissue after electrolytic and 980 nm laser induced lesions," *Proc SPIE Prog Ther Laser Appl Laser Tissue Interact.*, Vol. 5142, pp. 192–199, 2003.

18. Reinoso R.F., A.B. Telfer, M. Rowland, "Tissue water content in rats measured by desiccation," *Journal of Pharmacological and Toxicological Methods*, Vol. 38, pp. 87-92, 1997.

19. Gulsoy M., H.O. Tabakoglu, O. Bozkulak, A. Aksoy, R. Canbeyli, "Removal of brain tissue by electrolytic and laser coagulation techniques." *EMBEC'02 2nd european medical and biological engineering conference*, Vol. 3(2), pp. 986–987, 2002.

20. Goldman, L., *Lasers in Medicine*, Florida: CRC Press, 2002.

21. Germer, C.T., A. Roggan, J.P. Ritz, C. Isbert, D. Albrecht, G. Muller, H.J. Buhr, "Optical Properties of Native and Coagulated Human Liver Tissue and Liver Metastases in the Near Infrared Range." *Lasers in Surgery and Medicine*, Vol. 23, pp. 194–203, 1998.

22. Zhang, M., M.A. Yue-feng, G. Jian-xin, J. Guan-yu, X. Shan-xiangü, T. Xiang-luo, H. An, L. Jiao-kun, "Basic fibroblast growth factor alleviates brain injury following global ischemia reperfusion in rabbits." *Journal of Zhejiang University Science* Vol. 6B(7), pp. 637-643, 2005.

23. Ridge, J.W., "Resting and Stimulated Respiration in vitro in the Central Nervous System." Biochem. J. 105:831-835, 1967.

24. Roider, J, F Hillenkamp, T Flotte, and R Birngruber, "Microphotocoagulation: selective effects of repetitive short laser pulses." *Proc Natl Acad Sci U S A*. Vol. 90(18), pp. 8643–8647, September 1993.

25. Voorhees, M.E., B.F. Brian, "Blood-gas exchange devices." *Int. Anesthesiol. Clin*. Vol. 34(2), pp. 29-45, 1996.